Medicago truncatula MOT1.3 is a plasma membrane molybdenum transporter required for nitrogenase activity in root nodules.

Manuel Tejada-Jiménez[1,a,b], Patricia Gil-Díez[1], Javier León-Mediavilla[1], Jiangqi Wen[2], Kirankumar S. Mysore[2], Juan Imperial[1,3], Manuel González-Guerrero[1,a]

[1]Centro de Biotecnología y Genómica de Plantas (UPM-INIA). Campus de Montegancedo. Universidad Politécnica de Madrid. Crta. M-40 km 38. 28223 Pozuelo de Alarcón (Madrid). Spain.

[2]Plant Biology Division, The Samuel Roberts Noble Foundation, Ardmore, Oklahoma 73401.

[3]Consejo Superior de Investigaciones Científicas. Madrid. Spain.

[a]Corresponding authors: Manuel Tejada-Jiménez (q62tejim@uco.es), phone: +34 957218591; and Manuel González-Guerrero (manuel.gonzalez@upm.es), phone: +34 918334558

[b]Present address: Department of Biochemistry and Molecular Biology. Universidad de Córdoba. Campus de Rabanales. Edificio Severo Ochoa. Córdoba. Spain.

Total word count for the main text: 5932

Introduction word count:1033

Materials and Methods word count: 1245

Results word count: 1679

Discussion word count: 1776

Acknowledgements word count: 103

Number of Figures: 7 (6 in colour)

Number of Supporting information files: 1 Materials and Methods, 1 Figure Legends, 2 Tables, 12 Figures

Summary

- Molybdenum, as a component of the iron-molybdenum cofactor of nitrogenase, is essential for symbiotic nitrogen fixation. This nutrient has to be provided by the host plant through molybdate transporters.
- Members of the molybdate transporters family MOT1 were identified in the model legume *Medicago truncatula* and their expression in nodules determined. Yeast toxicity assays, confocal microscopy, and phenotypical characterization of a *Tnt1* insertional mutant line were carried out in the one *M. truncatula* MOT1 family member expressed specifically in nodules.
- Among the five MOT1 members present in *M. truncatula* genome, *MtMOT1.3* is the only one uniquely expressed in nodules. MtMOT1.3 shows molybdate transport capabilities when expressed in yeast. Immunolocalization studies revealed that MtMOT1.3 is located in the plasma membrane of nodule cells. A *mot1.3-1* knockout mutant showed an impaired growth concomitant with a reduction in nitrogenase activity. This phenotype was rescued by increasing molybdate concentrations in the nutritive solution, or upon addition of an assimilable nitrogen source. Furthermore, *mot1.3-1* plants transformed with a functional copy of *MtMOT1.3* showed a wild type-like phenotype.
- These data are consistent with a model in which MtMOT1.3 would be responsible for introducing molybdate into nodule cells, which will be later used to synthesize functional nitrogenase.

Keywords: symbiotic nitrogen fixation, molybdate transport, *Medicago truncatula*, nitrogenase, metal transport.

Introduction

Molybdenum is one of the scarcest oligonutrients in the biosphere (Esteifel, 2002). Plants use it as part of the molybdenum cofactor (Moco) in just five enzymes involved in nitrate assimilation, purine metabolism, phytohormone production, and sulfite detoxification (Tejada-Jimenez et al., 2013). This nutrient, unlike other transition metals, is recovered from soil as the oxyanion molybdate instead of a cationic form. This determines that the transporters involved in this process are not the classical ones required for iron, copper, or zinc uptake, but members of other families. Molybdate shares some physicochemical characteristics with sulfate leading to cross-inhibition of sulfate transport by molybdate, probably due to non-specific molybdate transport through sulfate transporters in plants (Stout et al., 1951). Therefore, until recently it was thought that sulfate transporters might mediate molybdate transport in eukaryotic systems (Mendel & Hansch, 2002; Kaiser et al., 2005). The only known plant-type specific molybdate transporters belong to the Molybdate Transporter type 1 (MOT1) family and were identified in parallel in the green alga *Chlamydomonas reinhardtii* (Tejada-Jimenez et al., 2007) and in the higher plant *Arabidopsis thaliana* (Tomatsu et al., 2007). They share a high degree of homology with the sulfate transport family SULTR, but lack the conserved STAS domain (Tejada-Jimenez et al., 2007). In *C. reinhardtii*, CrMOT1 is responsible for high-affinity molybdate uptake, a process that is not severely affected by sulfate, indicating that MOT1 proteins are molybdate-specific transporters (Tejada-Jimenez et al., 2007). In Arabidopsis two members of the MOT1 family have been identified. One of them has been proposed to play a role in efficient Mo uptake from the soil (Tomatsu et al., 2007), although this function is not clear given the conflicting subcellular localizations reported for this transporter in plasma membrane or in mitochondria (Tomatsu et al., 2007; Baxter et al., 2008); while a second member of the MOT1 family is located in the vacuole of leaves and seems to be involved in intracellular and inter-organ Mo transport (Gasber et al., 2011). More recently, a MOT1 protein (LjMOT1) has been identified in *Lotus japonicus*, with a role in molybdate uptake from soil and translocation to the shoots, being located in the plasma membrane when expressed in tobacco leaves (Gao et al., 2016). In addition, another molybdate transporter family, MOT2, belonging to the major facilitator superfamily has been identified in *C. reinhardtii* (Tejada-Jimenez et al., 2011), indicating that molybdate transporters have appeared at least twice in evolution. However, its functionality as molybdate transporters has only been proved in this alga.

100 While all the plants employ molybdenum for Moco biosynthesis, legumes have
101 an additional use for it. These organisms also require molybdenum for the assembly of
102 the iron-molybdenum cofactor (FeMoco) of nitrogenase (Georgiadis et al., 1992; Rubio
103 & Ludden, 2008), the enzyme responsible for nitrogen fixation in their root nodules. In
104 legumes, FeMoco is assembled by diazotrophic bacteria living within differentiated root
105 organs, the nodules. These organs are developed in a complex process starting with the
106 detection of rhizobial nodulation factors (Nod) by the host plant that leads to root hair
107 curling, bacteria trapping, hydrolysis of the plant cell wall and bacteria delivery to the
108 root nodule primordium through an infection thread (Kondorosi et al., 1984; Brewin,
109 1991; Oldroyd, 2013). Once in the plant cytoplasm, rhizobia together with a plant-
110 derived membrane result in organelle-like structures, the symbiosomes, where nitrogen
111 fixation takes place. Two different types of nodules can be found in legumes (Sprent,
112 2007): determinate and inderterminate nodules. In inderterminate nodules, as those
113 found in *Medicago truncatula*, the continuous meristem growth results in the formation
114 of at least four different zones in mature nodules: the meristematic zone that drives
115 nodule growth; the infection/differentiation zone, where rhizobia are released through
116 the infection thread and differentiates to bacteroids; the fixation zone where nitrogenase
117 carries out its enzymatic activity; and the senescent zone where bacteroids are degraded
118 (Vasse et al., 1990). An additional nodule zone, the interzone, can be defined as the
119 transition between infection/differentiation and fixation zone (Roux et al., 2014). Once
120 the oxygen tension drops in the interzone, endosymbiotic bacteroids express nitrogenase
121 and the machinery that allows them synthesize FeMoco. Among them, is the *modABC*
122 operon, responsible for molybdate uptake from the peribacteroid space (Maupin-Furlow
123 et al., 1995; Delgado et al., 2006; Hernandez et al., 2009). Consequently, for molybdate
124 to reach the bacteroids, it has to cross the plasma and the symbiosome membranes, a
125 process that has to be mediated by transporters belonging to two different families,
126 given the two different directions of transport required.
127 In spite of the essential role that molybdenum has in nitrogenase, and the
128 importance of nitrogenase in legume colonization of new environments and in
129 sustainable agriculture, the transporters involved in molybdenum supply to the nodule
130 cells are not known. It can be hypothesized that molybdate transfer could in some cases
131 be mediated by sulfate transporters. In this case, molybdate transfer across the
132 symbiosome membrane could be carried out by SST1-like proteins, that have been
133 previously associated with sulfate delivery to symbiosomes (Krusell et al., 2005). At the

134 plasma membrane, another sulfate transporter, such a SHST1 homologue could mediate
135 molybdate uptake by rhizobia-infected cells since this transporter from the legume
136 *Stylosanthes hamata* has already been shown to transport molybdate when it is
137 expressed in yeast (Fitzpatrick et al., 2008). However, *in planta* SHST1 is expressed in
138 the root and it is involved in sulfate uptake (Smith et al., 1995), while its relationship
139 with plant molybdate transport has not been determined yet. A more likely alternative
140 would be transporters from the MOT1 or MOT2 families, since they could finely tune
141 molybdate delivery for symbiotic nitrogen fixation, given their high specificity for this
142 anion.

143 In this work, we have identified a *M. truncatula* member of the MOT1 family
144 (MtMOT1.3) involved in molybdate transport to nodule cells. *MtMOT1.3* is specifically
145 expressed in nodules. Its protein product is located in the plasma membrane of infected
146 and non-infected cells in the fixation zone of the nodule, coinciding with the zone where
147 *MtMOT1.3* is expressed. *M. truncatula* plants lacking a functional *MtMOT1.3* gene
148 show a reduction of nitrogenase activity connecting MtMOT1.3 function with
149 molybdenum supply for FeMoCo biosynthesis. This is the first molybdate transporter
150 known to be specific of legume symbiotic nitrogen fixation.

151

152 **Materials and Methods**

153 Biological material and growth conditions

154 *M. truncatula* R108 seeds were scarified in the presence of concentrated sulfuric
155 acid for 7 min. Then, seeds were washed several times with cold water, surface
156 sterilized with 50 % (v/v) bleach for 90 s and incubated overnight with sterile water in
157 the dark. After 48 h at 4 ºC, seeds were germinated in water-agar plates 0.8 % (w/v).
158 Seedlings were transferred to sterile perlite pots or to Jenner's solution for hydroponic
159 growth (Brito et al., 1994), and inoculated with *Sinorhizobium meliloti* 2011 or the same
160 bacterial strain transformed pHC60 (Cheng & Walker, 1998). Plants were grown in a
161 greenhouse under 16 h light and 22 ºC. In the case of perlite pots, plants were watered
162 every two days with Jenner's solution or water alternatively. Nodules were collected 28
163 dpi. Plants growing under non-symbiotic conditions were supplemented every two
164 weeks with 2 mM KNO_3. *Agrobacterium rhizogenes* strain ARqua1 having the
165 appropriate vector was used for *M. truncatula* hairy-root transformation (Boisson-
166 Dernier et al., 2001). Agroinfiltration for transitory expression experiments were

167 performed in *N. benthamiana* leaves using *A. tumefaciens* C58C1 carrying the
168 corresponding genetic construct.
169 *Saccharomyces cerevisiae* strain 31019b (MATa *ura3 mep1Δ mep2Δ::LEU2*
170 *mep3Δ:: KanMX2*) was used for heterologous expression assays (Marini et al., 1997).
171 Yeasts were grown in synthetic dextrose (SD) or yeast peptone dextrose medium
172 supplemented with 2 % glucose (Sherman et al., 1986).
173
174 Quantitative real-time RT-PCR
175 Transcriptional expression studies were carried out by real-time RT-PCR
176 (StepOne plus, Applied Biosystems) using the Power SyBR Green master mix (Applied
177 Biosystems). Primers used are indicated in Supporting Information, Table S1. RNA
178 levels were normalized by using the *ubiquitin carboxy-terminal hydrolase* gene as
179 internal standard. RNA isolation and cDNA synthesis were carried out as previously
180 described (Tejada-Jimenez et al., 2015).
181
182 GUS Staining
183 *pMtMOT1.3::GUS* construct was obtained by amplifying 1.1 kb upstream of the
184 *MtMOT1.3* (Nakagawa et al., 2007) start codon using the primers 5MtMOT1.3pGW and
185 3MtMOT1.3pGW (Supporting Information, Table S1). The resulting fragment was
186 cloned by Gateway cloning technology (Invitrogen) into pGWB3 vector. Hairy-root
187 transformation was carried out as described above. GUS staining was performed in root
188 of 28-dpi plants as previously described (Vernoud et al., 1999). Nodules sections were
189 clarified with 50% bleach for 30 min.
190
191 Immunohistochemistry and confocal microscopy
192 A genomic region comprising *MtMOT1.3* full gene and 1.1 kb upstream of its
193 start codon was cloned into pGWB13 vector (Nakagawa et al., 2007) using Gateway
194 cloning technology (Invitrogen). The resulting genetic construct contains *MtMOT1.3*
195 gene under the control of its own promoter and with three C-terminal HA epitopes in
196 frame. Hairy-root transformation was carried out as indicated above. *M. truncatula*
197 transformed plants were inoculated with *S. meliloti* 2011 constitutively expressing GFP.
198 Nodules and roots were collected at 28-dpi and fixed at 4 ºC overnight in 4 % (w/v)
199 paraformaldehyde and 2.5 % (w/v) sucrose in phosphate-buffered saline (PBS). Fixed
200 plant material was sectioned, 100 µm wide, with a Vibratome 1000 Plus. Sections were

201 dehydrated by serial incubation with methanol (30 %, 50 %, 70 % and 100 % [v/v] in
202 PBS) for 5 min and then rehydrated following the same methanol series in reverse
203 order. Cell wall permeabilization was carried out by incubation with 2 % (w/v) cellulase
204 in PBS for 1 h and 0.1 % (v/v) Tween 20 for 15 min. Sections were blocked with 5 %
205 (w/v) bovine serum albumin in PBS and then incubated with 1:50 anti-HA mouse
206 monoclonal antibody (Sigma) in PBS at room temperature for 2 h. Primary antibody
207 was washed three times with PBS for 10 min and subsequently incubated with 1:40
208 Alexa594-conjugated anti-mouse rabbit monoclonal antibody (Sigma) in PBS at room
209 temperature for 1 h. Secondary antibody was washed three times with PBS for 10 min,
210 and then DNA was stained using DAPI. Images were obtained with a confocal laser-
211 scanning microscope (Leica SP8).
212
213 Transient expression in *Nicotiana benthamiana* leaves
214 MtMOT1.3 transient expression in tobacco leaves was carried out as previously
215 described (Voinnet et al., 2003). *MtMOT1.3* CDS was cloned into pGWB5 (Nakagawa
216 et al., 2007) by Gateway cloning technology (Invitrogen), resulting in C-terminal fusion
217 to GFP. *A. tumefaciens* C58C1 (Deblaere et al., 1985) cells independently transformed
218 with this construct, with the plasma membrane marker pm-CFP pBIN (Nelson et al.,
219 2007) or with the silencing suppressor p19 of *Tomato bushy stunt virus* (Voinnet et al.,
220 2003) were injected into 4-week-old *N. benthamiana* leaves. Expression of the
221 appropriate construct was analyzed after 3 d by confocal laser-scanning microscopy
222 (Leica).
223
224 Nitrogenase activity
225 Acetylene reduction assay was used to measure nitrogenase activity (Hardy et
226 al., 1968). Wild-type and mutant plants 28 dpi were separately introduced in 30-mL
227 tubes. Each tube was sealed with rubber stoppers and contained at least four
228 independently transformed plants. Three mililiters of air of each bottle was replaced by
229 the same volume of acetylene, tubes were subsequently incubated for 30 min at room
230 temperature. Produced ethylene was measured by analyzing 0.5 mL of gas from each
231 bottle in a Shimadzu GC-8A gas chromatograph using a Porapak N column.
232
233 Metal content determination

234 Inductively coupled plasma optical emission spectrometry was carried out at the
235 Unit of Metal Analysis in the Scientific and Technology Centers of the Universidad de
236 Barcelona (Spain).
237
238 Nitrate reductase activity
239 Nitrate reductase activity was analyzed as described by Scheible et al. (1997)
240 with some modifications. We started from 100 mg of fresh leaves. The extraction buffer
241 used for crude extracts preparation contained 100 mM potassium phosphate pH 7.5, 5
242 mM magnesium acetate, 10 % glycerol (v/v), 10 % polyvinylpolypyrrolidone (w/v), 0.1
243 % Triton X-100, 1 mM EDTA, 0.05 % ß-mercaptoethanol, 1 mM PMSF. Plant material
244 was homogenized with liquid nitrogen and 1:6 extraction buffer (v/v). The crude extract
245 was centrifuged at 14,000 x*g* at 4 ºC for 15 min. The reaction was initiated by adding
246 0.05 mL of crude extract to 0.5 mL of reaction buffer and incubated at 30 ºC for 20 min.
247 The reaction buffer contained 50 mM potassium phosphate pH 7.5, 10 mM KNO_3, 5
248 mM EDTA and 0.5 mM NADH. Nitrate reduction reaction was stopped by adding 1
249 volume of 1 % sulfanilamide in 2.4 M HCl, and 1 volume of 0.02 % N-1-naphtyl-
250 ethylenediamine. After centrifugation absorbance at 540 nm was measured in
251 UV/visible spectrophotometer Ultrospect 3300 pro (Amersham Bioscience).
252
253 Bioinformatics
254 Members of the MOT1 family in *M. truncatula* were identified by the Basic
255 Local Alignment Search Tool in the *M. truncatula* Genome Project database
256 (http://www.jcvi.org/medicago/index.php), using as reference sequence a member of the
257 MOT1 family from Arabidopsis (NP_180139). Protein sequence alignment and
258 unrooted tree visualization were performed with MEGA7 package
259 (http://www.megasoftware.net/) using ClustalW software and neighbor joining
260 algorithm. Accession numbers: *Arabidopsis thaliana* AtMOT1.1, NP_180139.1;
261 AtMOT1.2, NP_178147.1; AtSULTR1.1, NP_192602.1; AtSULTR2.1, NP_196580.1;
262 AtSULTR3.1, ANM64117.1; AtSULTR4.1, AED91910.1; *Brassica napus* BnMOT1.1,
263 XP_013709878.1; BnMOT1.3, XP_013667816.1; BnSULTR1.1, XP_013715602.1;
264 BnSULTR2.1, NP_001302517.1; BnSULTR3.1, XP_013737126.1; BnSULTR4.1,
265 XP_013667920.1; *Glycine max* GmMOT1.1, XP_003545516.1; GmMOT1.4,
266 KRH05029.1; GmMOT1.6, XP_003527804.1; GmMOT1.7, XP_003523708.1;
267 GmSULTR1.3, XP_006593569.1; GmSULTR2.1, XP_003531538.1; GmSULTR3.1,

268 XP_003521258.1; GmSULTR4.2, XP_003552670.1; *Lotus japonicus* LjMOT1.1,
269 AFK43331.1; LjMOT1.2, AJE26312.1; LjSST1, CAL36108.1; *Medicago truncatula*
270 MtMOT1.1, XP_013465770.1; MtMOT1.2, XP_013465776.1; MtMOT1.3,
271 XP_013460259.1; MtMOT1.4, XP_013454709.1; MtMOT1.5, XP_003603486.1;
272 MtSULTR1.1, XP_003614968.1; MtSAT1, XP_003602002.1; *Oryza sativa*
273 OsMOT1.1, XP_015650610.1; OsMOT1.2, XP_015621613.1; OsSULTR1.2
274 XP_015650733.1; OsSULTR2.1, ABF94445.1; OsSULTR3.1, BAS82415.1;
275 OsSULTR4.1, XP_015612472.1; *Phaseolus vulgaris* PvMOT1.1, XP_007161270.1;
276 PvMOT1.2, XP_007137089.1; PvMOT1.3, XP_007161272.1; PvMOT1.4,
277 XP_007135722.1; PvSULTR1.1, XP_007141140.1; PvSULTR2.1, XP_007163633.1;
278 PvSULTR3.1, XP_007162459.1; PvSULTR4.1, XP_007139276.1; *Vitis vinifera*
279 VvMOT1.1, XP_002281989.2; VvMOT1.2, XP_002285217.1; VvSULTR1.1,
280 XP_010664070.1; VvSULTR2.1, XP_010652824.1; VvSULTR3.1, XP_003632327.1;
281 VvSULTR4.2, XP_002282491.2.
282
283 Statistical tests
284 Data were analyzed by Student's unpaired t test to calculate statistical
285 significance of observed differences. Test results with p-values less than 0.05 were
286 considered as statistically significant.
287
288 **Results**
289 *MtMoT1.3* belongs to the molybdate transporter MOT1 family and is specifically
290 expressed in nodules.
291 Due to the possible role of MOT1 transporters in Mo supply for symbiotic
292 nitrogen fixation, we carried out a search for MOT1 members in the *M. truncatula*
293 genome. Five putative *M. truncatula* proteins were found (encoded by *Medtr1g010210*,
294 *Medtr1g010270*, *Medtr3g464210*, *Medtr4g011600* and *Medtr3g108190*) showing a
295 sequence identity between 51.4 % and 65.7 % with an Arabidopsis member of the
296 MOT1 family. These proteins were annotated as sulfate transporter-like proteins;
297 however, sequence comparison showed that they cluster with plant MOT1 proteins and
298 are more distant to sulfate transporters (SULTR) (Fig. 1a). Additionally, these proteins
299 also contain the two sequence motifs conserved in all MOT1 proteins (Tejada-Jimenez
300 et al., 2007) (Fig. 1b). Therefore, we named these proteins MtMOT1.1 to MtMOT1.5,
301 respectively. The number of MOT1 members present in *M. truncatula* contrasts with the

302 situation reported for Arabidopsis where only two MOT1 transporters are present
303 (Tomatsu et al., 2007; Baxter et al., 2008; Gasber et al., 2011). Analysis of the number
304 of MOT1 members in already sequenced plants showed that these proteins are present,
305 in average, in a higher number in legumes than in non-legumes plants (Supporting
306 Information, Table S2). This finding suggests a particular role of MOT1 proteins in
307 legumes, where an additional molybdenum sink is present: diazotrophic bacteria in root
308 nodules.

309 In order to study the possible relationship of the five putative MOT1 members of
310 *M. truncatula* with symbiotic nitrogen fixation, a transcriptional analysis of these genes
311 was carried out by real-time RT-PCR in plants during symbiotic association with *S.*
312 *meliloti* or in uninoculated plants fertilized with nitrogen. We found that *MtMOT1.3*
313 expression is restricted to the nodule (Fig. 1c and 1d), while transcripts from the other
314 four *MtMOT1* genes were also detected at varying levels in other organs of the analyzed
315 plants (Supporting Information, Fig. S1). These results strongly suggest an important
316 role of MtMOT1.3 in the nodule, likely in molybdate transport connected to symbiotic
317 nitrogen fixation. *MtMOT1.3* expression levels were not significantly affected by
318 molybdate concentration in the nutritive solution (Supporting Information, Fig. S2).
319

320 MtMOT1.3 is a molybdate transporter

321 All the MOT1 proteins reported so far mediate molybdate transport, in form of
322 the oxyanion molybdate, to the cytosol (Tejada-Jimenez et al., 2013). The high
323 sequence similarity that MtMOT1.3 shares with the already characterized molybdate
324 transporters suggests that this protein could also mediate molybdate transport in the
325 same direction. To test this hypothesis, *MtMOT1.3* was heterologously expressed in the
326 yeast *S. cerevisiae*. This yeast is a good model to study of Mo transporters since it is one
327 of the few organisms that do not use molybdenum, excluding any effect of endogenous
328 specific molybdate transport activity (Mendel & Bittner, 2006). Toxicity studies showed
329 that yeasts expressing *MtMOT1.3* exhibit a defective growth in synthetic dextrose (SD)
330 solid medium in the presence of 50 μM molybdate, compared with yeast transformed
331 with the empty vector pDR196, but no growth differences were observed with the
332 control when no additional molybdate was added to the growth medium (Fig. 2a).
333 Similar results were obtained in SD liquid medium by monitoring yeast growth along
334 the time (Fig. 2b; Supporting Information, Fig. S3). The toxic effect observed in yeast is
335 the likely result of molybdenum being transported and accumulated in the cell as a

336 result of MtMOT1.3 activity (Fig. 2c). This result supports the functionality of
337 MtMOT1.3 as molybdate transporter towards the cytosol.
338
339 *MtMOT1.3* is expressed in the plasma membrane of nodule cells of the interzone and
340 fixation zones
341 To investigate the role of MtMOT1.3 in molybdenum supply to the nodule, we
342 studied the tissue specific localization of *MtMOT1.3* expression. This was assessed by
343 analyzing the expression of the ß-glucoronidase (*gus*) gene under the control of 1.1 kb
344 of genomic DNA directly upstream of the *MtMOT1.3* starting codon, that was selected
345 as promoter. Using this genetic construct, GUS activity was found in the nodule
346 interzone, with the maximum in the area corresponding with the fixation zone (Fig. 3a
347 and 3b). This expression distribution within the nodule matches with the transcription
348 data available in the Symbimics database obtained by means of laser-capture
349 microdissection coupled to RNA sequencing (Roux et al., 2014), where *MtMOT1.3*
350 expression is mainly detected in the interzone and fixation zones (Fig. 3c).
351 Localization of MtMOT1.3 protein was also analyzed using an
352 immunohistochemical and confocal microscopy approach. *M. truncatula* plants were
353 transformed with a genetic construct comprising the genomic region of *MtMOT1.3*
354 fused in frame with three hemagglutinin (HA) epitopes in C-terminus (MtMOT1.3-HA),
355 under the control of the same promoter used for the GUS assay. The chimeric
356 MtMOT1.3-HA protein was detected (in the red channel) with a mouse anti-HA
357 antibody and an Alexa594-conjugated anti-mouse secondary antibody. Its position
358 within the nodule was traced by DNA staining using 4',6-diamino-phenylindole (DAPI)
359 (blue) and a *S. meliloti* strain constitutively expressing GFP (green). In agreement with
360 the GUS activity data, MtMOT1.3-HA was detected in the interzone and fixation zones
361 of the nodule (Fig. 4a to 4c). Particularly, MtMOT1.3-HA signal was found in the
362 periphery of infected and non-infected cells (Fig. 4d to 4f), fitting with plasma
363 membrane localization. This signal was not the result of autofluorescence, since
364 sections obtained from the same biological material, subjected to the same preparation
365 protocol with the exception of the incubation with the primary anti-HA antibody, did
366 not show any fluorescence in the Alexa594 emission spectrum (Supporting Information,
367 Fig. S4). Moreover, the specific peripheral distribution of MtMOT1.3-HA was also
368 observed using an Alexa488-conjugated secondary antibody in nodules containing m-
369 Cherry-expressing *S. meliloti* (Supporting Information, Fig. S5). No MtMOT1.3-HA

370 signal was detected by Western blot analyses in roots from nodulated plants (Supporting
371 Information, Fig. S6), consistent with the nodule-specifc expression data obtained by
372 real-time PCR. To confirm the subcellular localization of MtMOT1.3 in the plasma
373 membrane, its coding sequence fused to the green fluorescent protein (GFP) in C-
374 terminus was transiently expressed in *N. benthamiana* leaves together with a plasma
375 membrane marker fused to cyan fluorescent protein (CFP). MtMOT1.3 signal and
376 plasma membrane marker signal co-localized in *N. benthamiana* leaves cells expressing
377 both genetic constructs (Fig. 4g to 4i), supporting the localization of MtMOT1.3 in the
378 plasma membrane. However, no GFP or CFP signals were found in cells expressing
379 only the plasma membrane marker or MtMOT1.3, respectively (Supporting
380 Information, Fig. S7), thus ruling out any non-specific signal when both constructs are
381 co-expressed.
382
383 Lack of *MtMOT1.3* leads to a reduction of nitrogenase activity
384 In order to investigate the role of MtMOT1.3 in symbiotic nitrogen fixation, the
385 mutant line NF10801 (*mot1.3-1*) was identified by a reverse genetics screening (Cheng
386 et al., 2011; Cheng et al., 2014) from a *Transposable Element from N. tabacum* (*Tnt1*)
387 insertion mutant library (Tadege et al., 2008). The mutant *mot1.3-1* carries a *Tnt1*
388 insertion in the second exon of the *MtMOT1.3* gene at position +1782 from the starting
389 codon (Fig. 5a). *MtMOT1.3* transcripts were not detected in the homozygous *mot1.3-1*
390 mutant (Fig. 5b), therefore MtMOT1.3 activity is not present in this mutant line.
391 The phenotype of *mot1.3-1* was evaluated in symbiotic conditions, with nitrogen
392 fixation as the sole nitrogen source, and under low Mo availability. In these conditions,
393 *mot1.3-1* mutant showed a reduced growth rate compared with wild-type plants (Fig.
394 5c). Consequently, plant biomass was reduced in the *mot1.3-1* mutant by 70 % in shoots
395 and 55 % in roots (Fig. 5d). Nitrogenase activity was measured in *mot1.3-1* and wild-
396 type plants by the acetylene-reduction assay (Dilworth, 1966; Schöllhorn & Burris,
397 1966). *mot1.3-1* plants showed a reduction of 90 % in nitrogenase activity, as compared
398 to the activity measured in wild-type plants (Fig. 5e). On a per-nodule basis, *mot1.3-1*
399 plants had in average 24 % of the nitrogenase activity of the wild-type ones (Supporting
400 Information, Fig. S8). Nodulation was not affected in the *mot1.3-1* mutant, since
401 nodules were comparable to wild-type plants in terms of number and shape (Fig. 5f and
402 5g). Moreover, no differences in nodule anatomy, or nodulation kinetics were observed
403 between mutant and control plants (Supporting Information, Fig. S9). However, these

404 nodules were on average smaller than those from wild type plants (Fig. 5g; Supporting
405 Information, Fig. S10). In addition, nodule molybdenum content in *mot1.3-1* plants was
406 significantly higher than the control (Fig. 5h), indicative of a role on molybdenum
407 homeostasis in this organ. In order to investigate whether the phenotype of *mot1.3-1*
408 plants is caused by a shortage in molybdenum supply, these plants were watered with a
409 nutrient solution containing 5 µg/L ammonium heptamolybdate. Under molybdenum
410 sufficient conditions, *mot1.3-1* mutants exhibited a growth rate, biomass and
411 nitrogenase activity comparable to wild-type plants (Supporting Information, Fig. S10).
412 A similar result was obtained in hydroponics, a growth condition where molybdenum
413 concentrations can be better controlled (Supporting Information, Fig. S11).
414 Interestingly, no MOT1 family member was more highly expressed in *mot1.3-1* nodules
415 than in wild-type plants (Supporting Information, Fig. S12).
416 To validate that the phenotype observed was the result of the *Tnt1* insertion in
417 *MtMOT1.3, mot1.3-1* plants were transformed with *MtMOT1.3-HA* construct under its
418 own promoter (same genetic construct used for MtMOT1.3 immunolocalization assay).
419 Insertion of the mutated gene in the *mot1.3-1* mutant under low molybdenum conditions
420 also restored wild-type growth (Fig. 5a to 5e), supporting that mutation of *MtMOT1.3* is
421 responsible for this abnormal phenotype. In addition, it also validates the
422 immunofluorescence data, since without a wild type-like expression profile and
423 localization, no complementation would have been observed.
424 To check whether the lack of MtMOT1.3 activity could affect other processes in
425 the plant, the phenotype of *mot1.3-1* mutant was assayed under non-symbiotic
426 conditions, with nitrate as nitrogen source. In this situation, plant growth relies on the
427 activity of the molybdo-enzyme nitrate reductase to reduce nitrate to nitrite that will be
428 subsequently converted to ammonia and incorporated to amino acids by the glutamine
429 synthetase/glutamine synthase pathway (Bernard & Habash, 2009). In these conditions
430 *mot1.3-1* plants showed a phenotype similar to wild-type plants in terms of growth rate,
431 biomass and nitrate reductase activity, regardless of the Mo availability (Fig. 6).
432 Therefore, the function of MtMOT1.3 seems to be restricted to symbiotic conditions
433 when symbiotic nitrogen fixation has an important role in plant growth.
434
435 **Discussion**
436 Obtaining nitrogen from the atmosphere by biological nitrogen fixation is a
437 sustainable alternative to the intensive use of synthetic nitrogen fertilizers in agriculture

438 (Smil, 1999). Legumes are able to use atmospheric N_2 as nitrogen source by means of a
439 symbiotic association with nitrogen-fixing bacteria from the soil. They occupy 12-15%
440 of the world arable land (Graham & Vance, 2003). However, maintaining an adequate
441 nitrogen fixation rate involves a complex biological process that requires an efficient
442 nutrient supply from the plant to the rhizobia (Udvardi & Poole, 2013). Molybdenum
443 supply is critical for symbiotic nitrogen fixation since this oligonutrient is needed to
444 synthesize the enzyme nitrogenase, directly involved in the reduction of N_2 to produce
445 NH_4^+. In plants molybdenum is also present in other enzymes carrying out important
446 metabolic processes such as nitrate assimilation (nitrate reductase) or phytohormone
447 biosynthesis (aldehyde oxidase) (Tejada-Jimenez et al., 2013). Little is known about
448 how plants take up molybdate from the soil and redistribute it to the sink organs,
449 although members of the molybdate transport protein family MOT1 are very likely
450 involved in this process in Arabidopsis (Tomatsu et al., 2007; Baxter et al., 2008;
451 Gasber et al., 2011). However, their physiological role in molybdenum homeostasis is
452 still unclear. Less is known for molybdate nutrition in legumes, in spite of the
453 importance of molybdenum in symbiotic nitrogen fixation. Considering the renewed
454 interest and recent advances towards introducing nitrogen fixing abilities into non-
455 legumes (Charpentier & Oldroyd, 2010; Curatti & Rubio, 2014; Lopez-Torrejon et al.,
456 2016) and the need for a more sustainable agriculture (Foley et al., 2011), this gap of
457 our knowledge needs to be filled if we are to ensure proper delivery of molybdenum to
458 produce functional nitrogenase in new biological systems. The present work represents
459 a first but decisive step toward optimization of molybdate allocation for nitrogen
460 fixation, where we have identified a nodule-specific MOT1 member in *M. truncatula*
461 (MtMOT1.3) as responsible for molybdenum supply for symbiotic nitrogen fixation.
462 Legumes appear to have expanded the number of genes encoding MOT1
463 proteins in their genome in order to adapt to the presence of an additional molybdenum
464 sink, the root nodule, doubling the average copy number in monocots and other dicots.
465 This is in contrast to genes encoding Nramp transporters, some of which play an
466 essential role in iron transport in rhizobia-infected cells (Kaiser et al., 2003; Tejada-
467 Jimenez et al., 2015), where no significant increase in gene copy numbers were
468 observed. One possible explanation for this, based on the fact that few plant proteins use
469 molybdenum-based cofactors, is that MOT1 transporters are only expressed in very few
470 cell types, highly specialized in the physiological processes catalyzed by Moco or
471 FeMoco-dependent enzymes. If this hypothesis is right, nodule cells should express a

472 specific MOT1 transporter responsible for ensuring molybdenum supply for symbiotic
473 nitrogen fixation, as is the case for *MtMOT1.3* in *M. truncatula.*
474 *MtMOT1.3* is expressed in the nodule interzone and in the early fixation zone.
475 This transcription pattern is also validated by the transcriptomic data obtained from the
476 Symbimics database (Roux et al., 2014). This expression profile is consistent with a
477 situation in which the rhizobia-infected cell is increasing its molybdenum content to
478 transfer it to the bacteroids, so that when the physiological conditions are right, they can
479 start synthesizing FeMoco. In contrast, iron-transporting *MtNramp1*, responsible for
480 iron uptake by rhizobia-infected cells, shows a different expression profile, with a
481 maximum of expression in the infection/differentiation zone (Tejada-Jimenez et al.,
482 2015). This difference for the expression of iron and molybdenum transporter genes
483 indicates that the uptake of these two elements occurs in two separate moments during
484 nodule development, probably reflecting an earlier need for certain ferroproteins other
485 than nitrogenase. It also indicates that molybdate release from the vasculature for uptake
486 by rhizobia-infected cells occurs at the interzone and early fixation zone, in contrast to
487 what has been proposed for iron and other transition metals (Rodriguez-Haas et al.,
488 2013; González-Guerrero et al., 2014; González-Guerrero et al., 2016). However,
489 neither *MtMOT1.3* nor *MtNramp1* are expressed in the older parts of the fixation zone.
490 This suggests that no additional metal uptake is taking place in this zone, indicating
491 either a high degree of protein stability in the fixation zone, or an effective recycling of
492 essential metallic nutrients.
493 MtMOT1.3 is a plasma membrane-bound protein, as indicated by both the
494 immunolocalization of a HA-tagged fusion in *M. truncatula* nodules and the
495 colocalization studies of MtMOT1-GFP with a plasma membrane marker in tobacco
496 leaves. In Arabidopsis, while AtMOT1.2 is clearly localized in the vacuole of leaf cells
497 (Gasber et al., 2011), contradicting localization data have been reported for AtMOT1.1,
498 claiming either plasma membrane or mitochondrial localizations (Tomatsu et al., 2007;
499 Baxter et al., 2008). These conflicting data seem to be caused by the GFP marker fused
500 to AtMOT1.1, since when it is fused to the N-terminus of AtMOT1.1 it leads to plasma
501 membrane localization, while the C-terminus fusion results in mitochondrial
502 localization. Our MtMOT1.3 subcellular localization data have been obtained using two
503 different methodologies: immunolocalization in *M. truncatula* cells by detecting HA
504 epitope fused to MtMOT1.3, and transient expression in *N. benthamiana* fused to GFP.
505 Both approaches yielded the same result reinforcing MtMOT1.3 localization in the

506 plasma membrane. The observed immunofluorescence data are not the result of any
507 autofluorescence, since similar fluorescence profiles were observed using two different
508 fluorescent probes. Moreover, when no probe was added to the sections, no
509 fluorescence was detected in them, indicating that the signal was the result of the
510 antibody binding. There is no evidence of unspecific recognition of any epitope other
511 than the HA-tag in the Western blot analysis carried out using an anti-HA antibody.
512 Furthermore, previous data showed that the Alexa594-conjugated antibody used was
513 specific for HA-expressing proteins (Tejada-Jiménez et al., 2015). Finally, expressing
514 *MtMOT1.3-HA* in a *mot1.3-1* mutant background resulted in complementation and
515 recovery of the wild-type phenotype, which indicates that the tagged transporter is being
516 targeted to the proper subcellular compartment.

517 Like MOT1 family members, MtMOT1.3 transports molybdate towards the
518 cytosol, as indicated by the yeast toxicity assays. The phenotype characterization of a
519 *Tnt1* mutant line strongly suggests that this activity is used by *M. truncatula* to
520 introduce molybdate into nodule cells. The knockout mutant line *mot1.3-1* has lower
521 nitrogenase activity than wild-type control plants, both when whole plants or nodules
522 were compared. Consequently, plant growth is reduced due to lack of fixed nitrogen.
523 Nodules from *mot1.3-1* are on average smaller than those from wild-type plants. This is
524 not caused by a delayed nodulation, since nodulation kinetics are very similar to wild-
525 type plants. Neither it is due to a defect of the nodulation process, as the nodule
526 organization does not show any alteration in *mot1.3-1* nodules. Finally, the observed
527 reduction in nodule size (around 75% of wild type) cannot account for the observed
528 reduction in nodule nitrogenase activity (ca 25% of wild-type leves). Alternatively, it
529 could be hypothesized that the reduction in nodule size could be caused by the reduced
530 uptake of a nutrient essential for nodule functioning. The *mot1.3-1* phenotype is
531 molybdenum-dependent, since molybdate fortification of the nutritive solution resulted
532 in wild-type looking *mot1.3-1* plants, in apparent contradiction to the higher levels of
533 molybdenum detected in *mot1.3-1* nodules. This accumulation pattern has also been
534 observed when studying a nodule-specific plasma membrane copper transporter
535 (unpublished data). One possible explanation is the existence of a signal indicating
536 intracellular metal deficiency that would trigger more metal being transported to the
537 nodule. Since the uptake transporter is not present, this would result in metal
538 accumulation in the nodule apoplast and in the vasculature. In any case, the molybdate
539 transport capabilities shown in yeast, the alteration of molybdate homeostasis in

540 nodules, the reduction of a molybdate-dependent enzymatic activity in nodules, its
541 plasma membrane localization, and the restoration of a wild-type phenotype by
542 increasing molybdate concentrations in the nutritive solution, point out to a role of
543 MtMOT1.3 in molybdate uptake by nodule cells.

544 The phenotype reversal by increasing the molybdate content of the nutritive
545 solution is the result of other membrane transporters that at higher molybdate
546 concentrations could counterbalance the absence of MtMOT1.3 activity. In *M.*
547 *truncatula* all the MOT1 proteins are expressed within the nodule, although only
548 *MtMOT1.3* exhibited a nodule-specific transcription pattern. It could be argued that
549 another member of the MOT1 family could carry out this role. If this were the case, an
550 induction of its expression levels in *mot1.3-1* nodules would be expected. However, we
551 observe a slight reduction of their expression levels, suggesting a different role in
552 molybdenum homeostasis in nodules. Alternatively, sulfate transporters could also
553 compensate the lack of MtMOT1.3; for instance, the sulfate transporter SHST1 from the
554 legume *Stylosanthes hamata* is able to transport molybdate upon expression in *S.*
555 *cerevisiae* (Fitzpatrick et al., 2008). Furthermore, proteins of the MOT2 family have
556 been also related to molybdate transport in the green alga *C. reinhardtii* (Tejada-
557 Jimenez et al., 2011) and members of the MOT2 family are present in *M. truncatula*
558 genome. However according to the database Symbimics, none of SHST1 or MOT2 *M.*
559 *truncatula* orthologues are significantly expressed in nodules (Roux et al., 2014), which
560 indicates that either another MOT1 transporter carried out this role in spite of the
561 reduced expression levels, or a member of a yet-to-be-identified molybdate transporter
562 family would be supplementing MtMOT1.3 function.

563 Under non-symbiotic conditions, MtMOT1.3 does not play an essential role, as
564 indicated by its expression profile and by the lack of phenotype observed under these
565 conditions. Even when the plants require Moco-dependent nitrate reductase activity to
566 grow, no differences were observed between mutant and wild-type plants. These results
567 reinforce the hypothesis of specialization of a legume MOT1 transporter during
568 evolution to provide molybdenum for symbiotic nitrogen fixation.

569 In conclusion, molybdate transported by the host plant is released from the
570 vasculature into the apoplast of the interzone/early fixation zone (Fig. 7). From there,
571 MtMOT1.3 introduces molybdate into rhizobia-infected cells, as well as in the non-
572 infected ones within the nodule. The latter raises the question of why the non-infected
573 cells would require molybdenum. Possible explanations would be that they are being

prepared if they become infected, that they are buffering or storing molybdenum to be used later, or that this molybdenum is required to synthesize active Moco-dependent enzymes in these cells. Once in the cell cytosol, molybdate has to be transported across the symbiosome membrane. Since no molybdate-specific efflux system is known, it could be speculated that this role is carried out by a sulfate transporter specific of this membrane such as SST1, whose mutation has a severe impact on nitrogenase activity (Krusell et al., 2005). Once in the peribacteroid space, ModABC would introduce molybdate into the bacteroid (Delgado et al., 2006; Cheng et al., 2016).

Acknowledgments

This research was funded by a European Research Council Starting Grant (ERC-2013-StG-335284), to MGG. Development of *M. truncatula Tnt1* mutant population was, in part, funded by the National Science Foundation, USA (DBI-0703285) to KSM. We would like to thank Dr. T. Coque and Dr. A. SanMillán (Ramón y Cajal Health Research Institute) for allowing us to use their Bioscreen equipment; and Dr. J. M. Argüello for sending us the mCherry-expressing *S. meliloti*. We would also like to acknowledge the other members of Laboratory 281 at Centro de Biotecnología y Genómica de Plantas (UPM-INIA) for their support and feedback in preparing this manuscript.

Author contribution

MTJ carried out most of the experiments. PGD performed the confocal microscopy using the anti-HA Alexa488-conjugated antibody, the nodule development cross-section, and the molybdenum content in nodules. JLM carried out the expression of MOT1 genes in the *mot1.3-1* mutant, as well as studied the effecto of molybdate concentrations in transcription levels. Both PGD and JLM studied the nodulation process in wild type and *mot1.3-1* plants over time. JW and KSM performed *Medicago truncatula* mutant screening and isolated the *mot1.3-1* allele. MTJ, JI, and MGG designed the experiments, analyzed the data and wrote the article.

608 **References**

609 **Baxter I, Muthukumar B, Park HC, Buchner P, Lahner B, Danku J, Zhao K, Lee**
610 **J, Hawkesford MJ, Guerinot ML, Salt DE. 2008**. Variation in molybdenum content
611 across broadly distributed populations of *Arabidopsis thaliana* is controlled by a
612 mitochondrial molybdenum transporter (MOT1). *PLoS Genetics* **4**: e1000004.

613 **Bernard SM, Habash DZ. 2009**. The importance of cytosolic glutamine synthetase in
614 nitrogen assimilation and recycling. *New Phytologist* **182**: 608-620.

615 **Boisson-Dernier A, Chabaud M, Garcia F, Becard G, Rosenberg C, Barker DG.**
616 **2001**. *Agrobacterium rhizogenes*-transformed roots of *Medicago truncatula* for the
617 study of nitrogen-fixing and endomycorrhizal symbiotic associations. *Molecular Plant-*
618 *Microbe Interactions* **14**: 695-700.

619 **Brewin NJ. 1991**. Development of the legume root nodule. *Annual Review of Cell*
620 *Bioloy* **7**: 191-226.

621 **Brito B, Palacios JM, Hidalgo E, Imperial J, Ruiz-Argueso T. 1994**. Nickel
622 availability to pea (*Pisum sativum* L.) plants limits hydrogenase activity of *Rhizobium*
623 *leguminosarum* bv. *viciae* bacteroids by affecting the processing of the hydrogenase
624 structural subunits. *Journal of Bacteriology* **176**: 5297-5303.

625 **Charpentier M, Oldroyd G. 2010**. How close are we to nitrogen-fixing cereals?
626 *Current Opinion in Plant Biology* **13**: 556-564.

627 **Cheng G, Karunakaran R, East AK, Poole PS. 2016**. Multiplicity of sulfate and
628 molybdate transporters and their role in nitrogen fixation in *Rhizobium leguminosarum*
629 bv. *viciae* Rlv3841. *Molecular Plant- Microbe Interactions* **29**: 143-152.

630 **Cheng HP, Walker GC. 1998**. Succinoglycan is required for initiation and elongation
631 of infection threads during nodulation of alfalfa by *Rhizobium meliloti. Journal of*
632 *Bacteriology* **180**: 5183-5191.

633 **Cheng X, Wen J, Tadege M, Ratet P, Mysore KS. 2011**. Reverse genetics in
634 *Medicago truncatula* using *Tnt1 i*nsertion mutants. *Methods in Molecular Biology* **678**:
635 179-190.

636 **Cheng X, Wang M, Lee HK, Tadege M, Ratet P, Udvardi M, Mysore KS, Wen J.**
637 **2014**. An efficient reverse genetics platform in the model legume *Medicago truncatula*.
638 *New Phytologist* **201**: 1065-1076.

639 **Curatti L, Rubio LM. 2014**. Challenges to develop nitrogen-fixing cereals by direct
640 nif-gene transfer. *Plant Science* **225**: 130-137.

641 **Deblaere R, Bytebier B, De Greve H, Deboeck F, Schell J, Van Montagu M,**
642 **Leemans J. 1985**. Efficient octopine Ti plasmid-derived vectors for Agrobacterium-
643 mediated gene transfer to plants. *Nucleic Acids Research* **13**: 4777-4788.
644 **Delgado MJ, Tresierra-Ayala A, Talbi C, Bedmar EJ. 2006**. Functional
645 characterization of the *Bradyrhizobium japonicum modA* and *modB* genes involved in
646 molybdenum transport. *Microbiology* **152**: 199-207.
647 **Dilworth MJ. 1966**. Acetylene reduction by nitrogen-fixing preparations from
648 *Clostridium pasteurianum*. *Biochimica et Biophysica Acta* **127**: 285-294.
649 **Esteifel EI. 2002**. Molybdenum and tungsten: their roles in biological processes. In:
650 Sigel A, Sigel H, eds. *Metal ions in biological systems* New York: Marcel Dekker Inc.,
651 1-30.
652 **Fitzpatrick KL, Tyerman SD, Kaiser BN. 2008**. Molybdate transport through the
653 plant sulfate transporter SHST1. *FEBS Letters* **582**: 1508-1513.
654 **Foley JA, Ramankutty N, Brauman KA, Cassidy ES, Gerber JS, Johnston M,**
655 **Mueller ND, O'Connell C, Ray DK, West PC, et al. 2011**. Solutions for a cultivated
656 planet. *Nature* **478**: 337-342.
657 **Gao JS, Wu FF, Shen SL, Meng Y, Cai YP, Lin Y. 2016**. A putative molybdate
658 transporter LjMOT1 is required for molybdenum transport in *Lotus japonicus*.
659 *Physiologia Plantarum*. **158**: 331-340.
660 **Gasber A, Klaumann S, Trentmann O, Trampczynska A, Clemens S, Schneider S,**
661 **Sauer N, Feifer I, Bittner F, Mendel RR, et al. 2011**. Identification of an Arabidopsis
662 solute carrier critical for intracellular transport and inter-organ allocation of molybdate.
663 *Plant Biology* **13**: 710-718.
664 **Georgiadis MM, Komiya H, Chakrabarti P, Woo D, Kornuc JJ, Rees DC. 1992**.
665 Crystallographic structure of the nitrogenase iron protein from *Azotobacter vinelandii*.
666 *Science* **257**: 1653-1659.
667 **González-Guerrero M, Matthiadis A, Saez A, Long TA. 2014**. Fixating on metals:
668 new insights into the role of metals in nodulation and symbiotic nitrogen fixation.
669 *Frontiers in Plant Science* **5**: 45.
670 **González-Guerrero M, Escudero V, Saez A, Tejada-Jimenez M. 2016**. Transition
671 metal transport in plants and associated endosymbionts: Arbuscular mycorrhizal fungi
672 and rhizobia. *Frontiers in Plant Science* **7**: 1088.
673 **Graham PH, Vance CP. 2003**. Legumes: importance and constraints to greater use.
674 *Plant Physiology* **131**: 872-877.

675 **Hardy RW, Holsten RD, Jackson EK, Burns RC. 1968**. The acetylene-ethylene assay
676 for n(2) fixation: laboratory and field evaluation. *Plant Physiology* **43**: 1185-1207.
677 **Hernandez JA, George SJ, Rubio LM. 2009**. Molybdenum trafficking for nitrogen
678 fixation. *Biochemistry* **48**: 9711-9721.
679 **Kaiser BN, Gridley KL, Ngaire Brady J, Phillips T, Tyerman SD. 2005**. The role of
680 molybdenum in agricultural plant production. *Annals of Botany* **96**: 745-754.
681 **Kaiser BN, Moreau S, Castelli J, Thomson R, Lambert A, Bogliolo S, Puppo A,**
682 **Day DA. 2003**. The soybean NRAMP homologue, GmDMT1, is a symbiotic divalent
683 metal transporter capable of ferrous iron transport. *Plant Journal* **35**: 295-304.
684 **Kondorosi E, Banfalvi Z, Kondorosi A. 1984**. Physical and genetic analysis of a
685 symbiotic region of *Rhizobium meliloti*: identification of nodulation genes. *Molecular*
686 *General Genetics* **193**: 445-452.
687 **Krusell L, Krause K, Ott T, Desbrosses G, Kramer U, Sato S, Nakamura Y,**
688 **Tabata S, James EK, Sandal N, et al. 2005**. The sulfate transporter SST1 is crucial for
689 symbiotic nitrogen fixation in *Lotus japonicus* root nodules. *Plant Cell* **17,** 1625-1636.
690 **Lopez-Torrejon G, Jimenez-Vicente E, Buesa JM, Hernandez JA, Verma HK,**
691 **Rubio LM. 2016**. Expression of a functional oxygen-labile nitrogenase component in
692 the mitochondrial matrix of aerobically grown yeast. *Nature Communications* **7**: 11426.
693 **Marini AM, Soussi-Boudekou S, Vissers S, Andre B. 1997**. A family of ammonium
694 transporters in *Saccharomyces cerevisiae*. *Molecular and Cellular Biology* **17**: 4282-
695 4293.
696 **Maupin-Furlow JA, Rosentel JK, Lee JH, Deppenmeier U, Gunsalus RP,**
697 **Shanmugam KT. 1995**. Genetic analysis of the *modABCD* (molybdate transport)
698 operon of *Escherichia coli*. *Journal of Bacteriology* **177**: 4851-4856.
699 **Mendel RR, Hansch R. 2002**. Molybdoenzymes and molybdenum cofactor in plants.
700 *Journal of Experimental Botany* **53**: 1689-1698.
701 **Mendel RR, Bittner F. 2006**. Cell biology of molybdenum. *Biochimimica et*
702 *Biophysica Acta* **1763**: 621-635.
703 **Nakagawa T, Kurose T, Hino T, Tanaka K, Kawamukai M, Niwa Y, Toyooka K,**
704 **Matsuoka K, Jinbo T, Kimura T. 2007**. Development of series of gateway binary
705 vectors, pGWBs, for realizing efficient construction of fusion genes for plant
706 transformation. *Journal of Bioscience and Bioengineering* **104**: 34-41.

707 **Nelson BK, Cai X, Nebenfuhr A. 2007**. A multicolored set of in vivo organelle
708 markers for co-localization studies in Arabidopsis and other plants. *Plant Journal* **51**:
709 1126-1136.
710 **Oldroyd GE. 2013**. Speak, friend, and enter: signalling systems that promote beneficial
711 symbiotic associations in plants. *Nature Reviews Microbiology* **11**: 252-263.
712 **Rodriguez-Haas B, Finney L, Vogt S, González-Melendi P, Imperial J, González-**
713 **Guerrero, M. 2013**. Iron distribution through the developmental stages of *Medicago*
714 *truncatula* nodules. *Metallomics* **5**: 1247-1253.
715 **Roux B, Rodde N, Jardinaud MF, Timmers T, Sauviac L, Cottret L, Carrere S,**
716 **Sallet E, Courcelle E, Moreau S, et al. 2014**. An integrated analysis of plant and
717 bacterial gene expression in symbiotic root nodules using laser-capture microdissection
718 coupled to RNA sequencing. *Plant Journal* **77**: 817-837.
719 **Rubio LM, Ludden PW. 2008**. Biosynthesis of the iron-molybdenum cofactor of
720 nitrogenase. *Annual Review of Microbiology* **62**: 93-111.
721 **Scheible WR, Gonzalez-Fontes A, Morcuende R, Lauerer M, Geiger M, Glaab J,**
722 **Gojon A, Schulze ED, Stitt M. 1997**. Tobacco mutants with a decreased number of
723 functional nia genes compensate by modifying the diurnal regulation of transcription,
724 post-translational modification and turnover of nitrate reductase. *Planta* **203**: 304-319.
725 **Schöllhorn R, Burris RH. 1966**. Study of intermediates in nitrogen fixation.
726 *Federation Proceedings* **25**: 710.
727 **Sherman F, Fink GR, Hicks JB. 1986**. *Methods in yeast genetics.* Plainview, NY:
728 Cold Spring Harbor Lab Press.
729 **Smil V. 1999**. Nitrogen in crop production: An account of global flows. *Global*
730 *Biogeochemical cycles* **13**: 647-662.
731 **Smith FW, Ealing PM, Hawkesford MJ, Clarkson DT. 1995**. Plant members of a
732 family of sulfate transporters reveal functional subtypes. *Proceedings of the National*
733 *Academy of Sciences, USA* **92**: 9373-9377.
734 **Sprent JI. 2007**. Evolving ideas of legume evolution and diversity: a taxonomic
735 perspective on the occurrence of nodulation. *New Phytologist* **174**: 11-25.
736 **Stout PR, Meagher WR, Pearson GA, Johnson CM. 1951**. Molybdenum nutrition of
737 crop plants: I. The influence of phosphate and sulfate on the absortion of molybdenum
738 from soils and solution cultures. *Plant and Soil* **3**: 51-87.

739 **Tadege M, Wen J, He J, Tu H, Kwak Y, Eschstruth A, Cayrel A, Endre G, Zhao**
740 **PX, Chabaud M, et al. 2008**. Large-scale insertional mutagenesis using the Tnt1
741 retrotransposon in the model legume *Medicago truncatula*. *Plant Journal* **54**: 335-347.
742 **Tejada-Jimenez M, Galvan A, Fernandez E. 2011**. Algae and humans share a
743 molybdate transporter. *Proceedings of the National Academy of Sciences, USA* **108**:
744 6420-6425.
745 **Tejada-Jimenez M, Llamas A, Sanz-Luque, E, Galvan A, Fernandez E 2007**. A
746 high-affinity molybdate transporter in eukaryotes. *Proceedings of the National Academy*
747 *of Sciences, USA* **104,** 20126-20130.
748 **Tejada-Jimenez M, Chamizo-Ampudia A, Galvan, A, Fernandez E, Llamas A.**
749 **2013**. Molybdenum metabolism in plants. *Metallomics* **5,** 1191-1203.
750 **Tejada-Jimenez M, Castro-Rodriguez R, Kryvoruchko I, Lucas MM, Udvardi M,**
751 **Imperial J, González-Guerrero M. 2015**. *Medicago truncatula* natural resistance-
752 associated macrophage Protein1 is required for iron uptake by rhizobia-infected nodule
753 cells. *Plant Physiology* **168**: 258-272.
754 **Tomatsu H, Takano J, Takahashi H, Watanabe-Takahashi A, Shibagaki N,**
755 **Fujiwara T. 2007**. An *Arabidopsis thaliana* high-affinity molybdate transporter
756 required for efficient uptake of molybdate from soil. *Proceedings of the National*
757 *Academy of Sciences, USA* **104**: 18807-18812.
758 **Udvardi M, Poole PS. 2013**. Transport and metabolism in legume-rhizobia symbioses.
759 *Annual Review of Plant Biology* **64**: 781-805.
760 **Vasse J, Billy F, Camut S, Truchet G. 1990**. Correlation between ultrastructural
761 differentiation of bacteroids and nitrogen fixation in alfalfa nodules. *Journal of*
762 *Bacteriology* **172**: 4295-4306.
763 **Vernoud V, Journet EP, Barker DG. 1999**. MtENOD20, a Nod factor-inducible
764 molecular marker for root cortical cell activation. *Molecular Plant-Microbe Interactions*
765 **12**: 604-614.
766 **Voinnet O, Rivas S, Mestre P, Baulcombe D. 2003**. An enhanced transient expression
767 system in plants based on suppression of gene silencing by the p19 protein of tomato
768 bushy stunt virus. *Plant Journal* **33**: 949-956.
769
770
771
772

773 **Figure Legends**

774

775 **Figure 1.** MtMOT1.3 is a member of the MOT1 protein and is expressed in the nodule.
776 (a) Unrooted tree of the plant SULTR and MOT1 families. (b) Alignment of the
777 conserved motifs of the MOT1 proteins present in all *M. truncatula* MOT1 members.
778 Sequences were aligned using ClustalW method and it is extracted from a larger
779 alignment including the full protein sequence of the *M. truncatula* MOT1 members. (c)
780 Determination of *MtMOT1.3* expression in nodulated and nitrogen-fertilized *M.*
781 *truncatula* plants relative to the internal standard gene Ubiquitin carboxyl-terminal
782 hydrolase. Data are the mean ± SD of two independent experiments with 4 pooled
783 plants. n.d., non-detected. (d) *MtMOT1.3* expression in nodulated and nitrogen-fertilized
784 *M. truncatula* plants. *Ubiquitin carboxyl-terminal hydrolase1* (*MtUb1*) was used as
785 control for PCR amplifications.

786

787 **Figure 2.** MtMOT1.3 transports molybdate towards the cytosol. (a) *S. cerevisiae* strain
788 31019b was transformed with PDR196 empty vector or PDR196 containing *MtMOT1.3*
789 coding sequence, and grown at 28 ºC for 3d in serial dilution (10X) on SD solid
790 medium medium without an added molybdenum source or containing 50 µM sodium
791 molybdate. (b) *S. cerevisiae* strains used in (a) were grown in SD liquid medium, with
792 and without 50µM sodium molybdate, at 28 ºC for 42 h. Yeast growth was monitored
793 by measuring optical density at 600 nm every 3h. (c) Molybdenum content in the yeast
794 grown in (b) after 42 h. Data are the mean ± SD of two independent experiments.

795

796 **Figure 3.** *MtMOT1.3* gene is expressed in the interzone and fixation zone of *M.*
797 *truncatula* nodules. (a) and (b) GUS staining of *M. truncatula* 28-dpi nodules
798 transiently expressing *gus* gene under the control of *MtMOT1.3* promoter. (a) Intact
799 nodule. (b) Longitudinal nodule section. Bars = 200 µm. (c) Expression of *MtMOT1.3*
800 in *M. truncatula* nodules by laser-capture microdissection coupled to RNA sequencing.
801 Data were obtained from the Symbimics database
802 (https://iant.toulouse.inra.fr/symbimics/). Meris, meristem; Infec, infection zone; Differ,
803 differentiation zone; Inter, interzone; Fix, fixation zone.

804

805 **Figure 4.** MtMOT1.3 is localized in the plasma membrane. (a) to (c) Cross section of a
806 28-dpi *M. truncatula* nodule transiently expressing MtMOT1.3-HA construct and

807 infected with a *S. meliloti* strain constitutively expressing GFP (green). MtMOT1.3-HA
808 was detected using an Alexa-594-conjugated antibody (red). (a) MtMOT1.3-HA signal.
809 (b) Overlay of MtMOT1.3-HA and *S. meliloti* signals. (c) Overlay of MtMOT1.3-HA
810 signal and differential interference contrast. a, meristem; b, infection/differentiation; c,
811 interzone; b, fixation. Bars = 200 µm. (d) to (f) Closer view in the fixation zone of M.
812 truncatula nodules. DNA was stained using DAPI (blue). (d) MtMOT1.3-HA signal. (e)
813 *S. meliloti* signal. (f) Overlay of MtMOT1.3-HA, *S. meliloti* and DNA signals. Bars =
814 50 µm. (g) to (i) Transient co-expression of MtMOT1.3-GFP and plasma membrane
815 marker-CFP in *N. benthamiana* leaves. (g) MtMOT1.3-GFP signal. (h) Plasma
816 membrane marker-CFP signal. (i) Overlay of MtMOT1.3-GFP, plasma membrane
817 marker-CFP signals and differential interference contrast. Bars = 25 µm.
818
819 **Figure 5.** *MtMOT1.3* mutation results in a reduced nitrogen fixation rate. (a) Position of
820 the *Tnt1* insertion within the *MtMOT1.3* genomic region. (b) RT-PCR amplification of
821 *MtMOT1.3* transcript in 28 dpi nodules of *M. truncatula* wild type (WT) and mutant
822 (*mot1.3-1*) plants. *Ubiquitin carboxyl-terminal hydrolase1* (*MtUb1*) was used as control
823 for PCR amplifications. (c) Growth of representative plants of wild type, *mot1.3-1*
824 mutant and *mot1.3-1* mutant transformed with the *MtMOT13-HA* construct. Bar = 3 cm.
825 (d) Dry weight of shoots and roots. Data are the mean ± SD of at least 6 independently
826 transformed plants. Asterisk indicates significant differences: $^{**}p < 0.01$, $^{***}p < 0.005$.
827 (e) Nitrogenase activity in 28-dpi nodules. Acetylene reduction was measured in
828 duplicate from two sets of four pooled plants. Data are the mean ± SD. (f) Number of
829 nodules per plant. Data are the mean ± SD of at least 6 independently transformed
830 plants. (g) Representative nodules of each *M. truncatula* line. Bar = 500 µm. (h)
831 Molybdenum content in shoots, roots, and nodules of wild type, *mot1.3-1* mutant, and
832 *mot1.3-1* mutant transformed with the *MtMOT13-HA* construct. Data are the mean ± SD
833 of 3 sets of 4 pooled plants.
834
835 **Figure 6.** *mot1.3-1* mutant phenotype is not present in non-symbiotic conditions. (a)
836 Growth of representative plants of wild type and *mot1.3-1* mutant. Bar = 3 cm. (b) Dry
837 weight of shoots and roots. Data are the mean ± SD of at least 8 independent plants. (c)
838 Nitrate reductase activity. Nitrate reduction was measured in duplicate. Data are the
839 mean ± SD.
840

841 **Figure 7.** Proposed model for MtMOT1.3 function in molybdenum homeostasis in *M.*
842 *truncatula*. Molybdenum, in form of molybdate would be released in the
843 infection/differentiation zone, as already described for iron, in a process that could be
844 assisted by a yet-to-be identified transporter that might belong to the MOT1 family
845 (MtMOT1.X). From this point MtMOT1.3 would introduce molybdate into the
846 cytoplasm of infected and non-infected cells within the nodule. The molybdate transport
847 across the symbiosome membrane could be mediated by an orthologue of *L. japonicus*
848 sulfate transporter SST1. Finally, molybdate would entry the bacteroids through the
849 membrane component of the bacterial high affinity molybdate transport system ModB.
850 IM, bacteroid inner membrane; OM, bacteroid outer membrane; SM, symbiosome
851 membrane; PM, nodule cell plasma membrane.
852
853
854
855
856

Figure 1

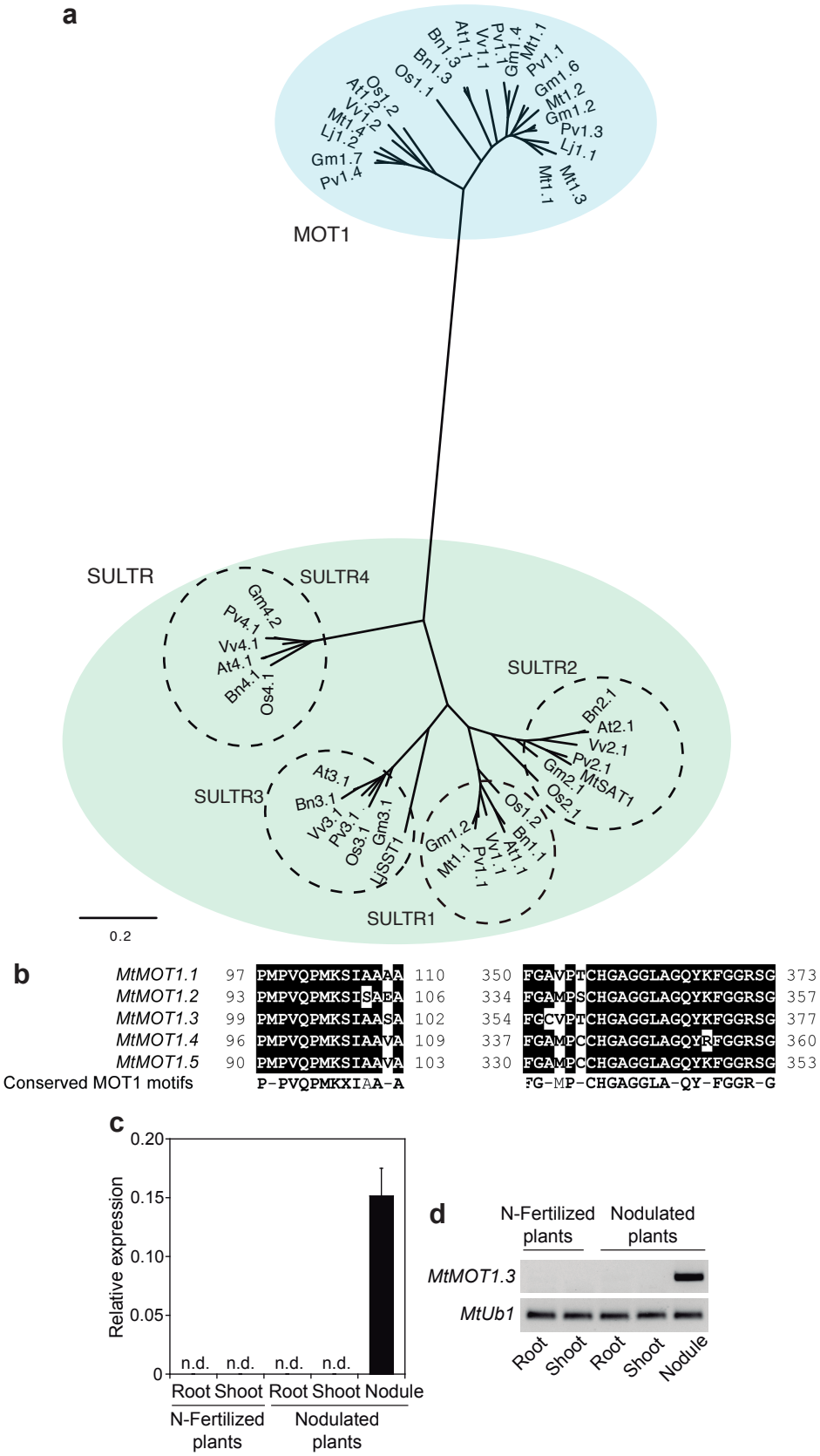
a
MOT1
SULTR
SULTR4
SULTR2
SULTR3
SULTR1
0.2
b
MtMOT1.1 97 PMPVQPMKSIAAAA 110 350 FGAVPTCHGAGGLAGQYKFGGRSG 373
MtMOT1.2 93 PMPVQPMKSISAEA 106 334 FGAMPSCHGAGGLAGQYKFGGRSG 357
MtMOT1.3 99 PMPVQPMKSIAASA 102 354 FGCVPTCHGAGGLAGQYKFGGRSG 377
MtMOT1.4 96 PMPVQPMKSIAAVA 109 337 FGAMPCCHGAGGLAGQYRFGGRSG 360
MtMOT1.5 90 PMPVQPMKSIAAVA 103 330 FGAMPCCHGAGGLAGQYKFGGRSG 353
Conserved MOT1 motifs P-PVQPMKXIAA-A FG-MP-CHGAGGLA-QY-FGGR-G
c
Relative expression
0.20
0.15
0.10
0.05
0
n.d. n.d. n.d. n.d.
Root Shoot Root Shoot Nodule
N-Fertilized plants
Nodulated plants
d
N-Fertilized plants
Nodulated plants
MtMOT1.3
MtUb1
Root Shoot Root Shoot Nodule

Figure 2

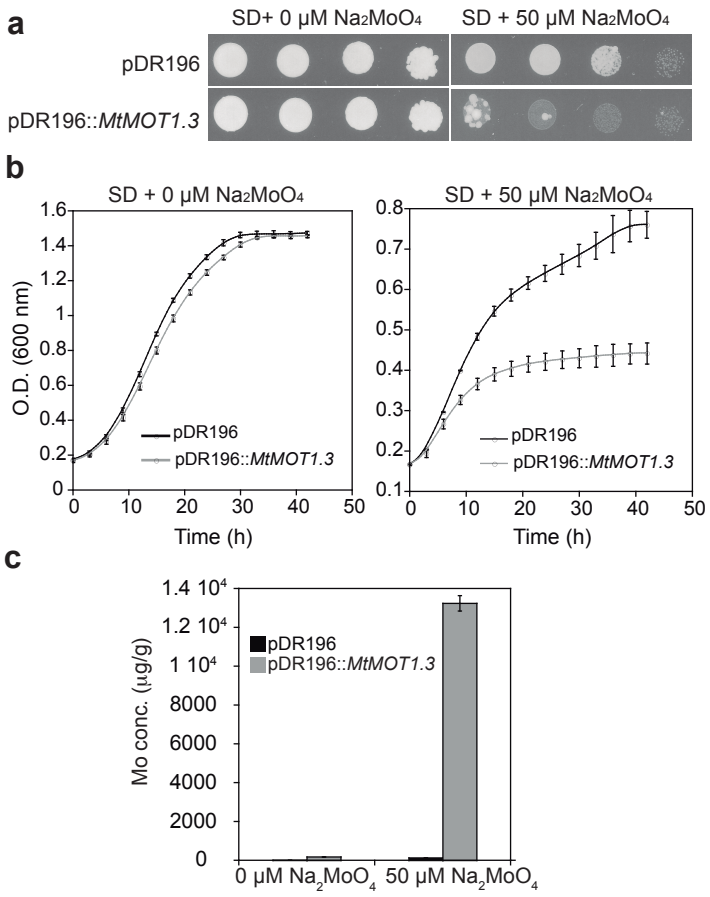
a
SD+ 0 μM Na2MoO4
SD + 50 μM Na2MoO4
pDR196
pDR196::MtMOT1.3
b
SD + 0 μM Na2MoO4
SD + 50 μM Na2MoO4
O.D. (600 nm)
Time (h)
pDR196
pDR196::MtMOT1.3
c
Mo conc. (μg/g)
pDR196
pDR196::MtMOT1.3
0 μM Na2MoO4
50 μM Na2MoO4

Figure 3

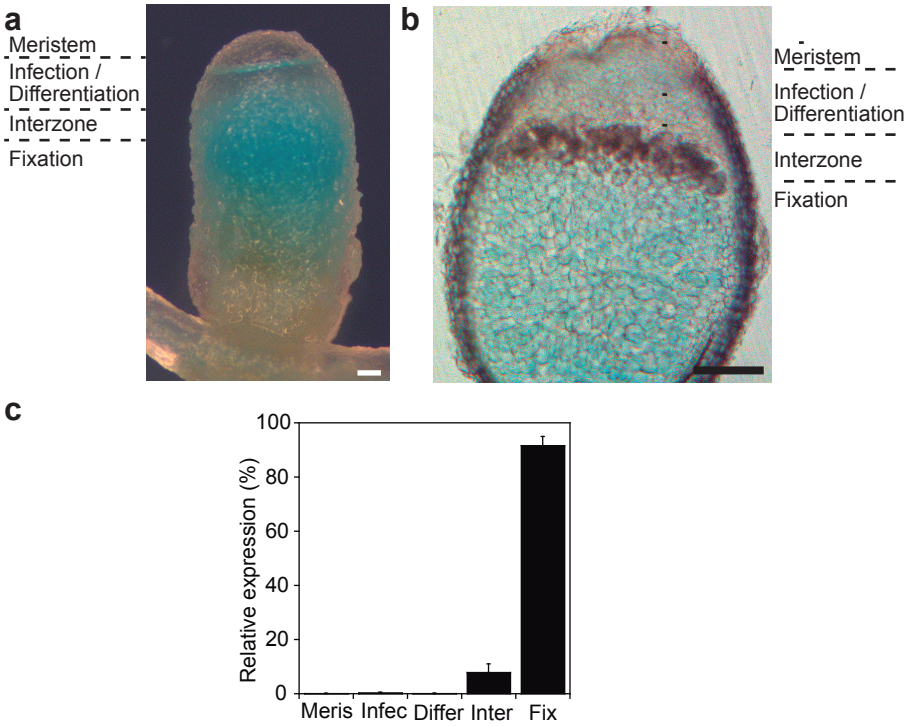
a
Meristem
Infection /
Differentiation
Interzone
Fixation
b
Meristem
Infection /
Differentiation
Interzone
Fixation
c
Relative expression (%)
100
80
60
40
20
0
Meris
Infec
Differ
Inter
Fix

Figure 4

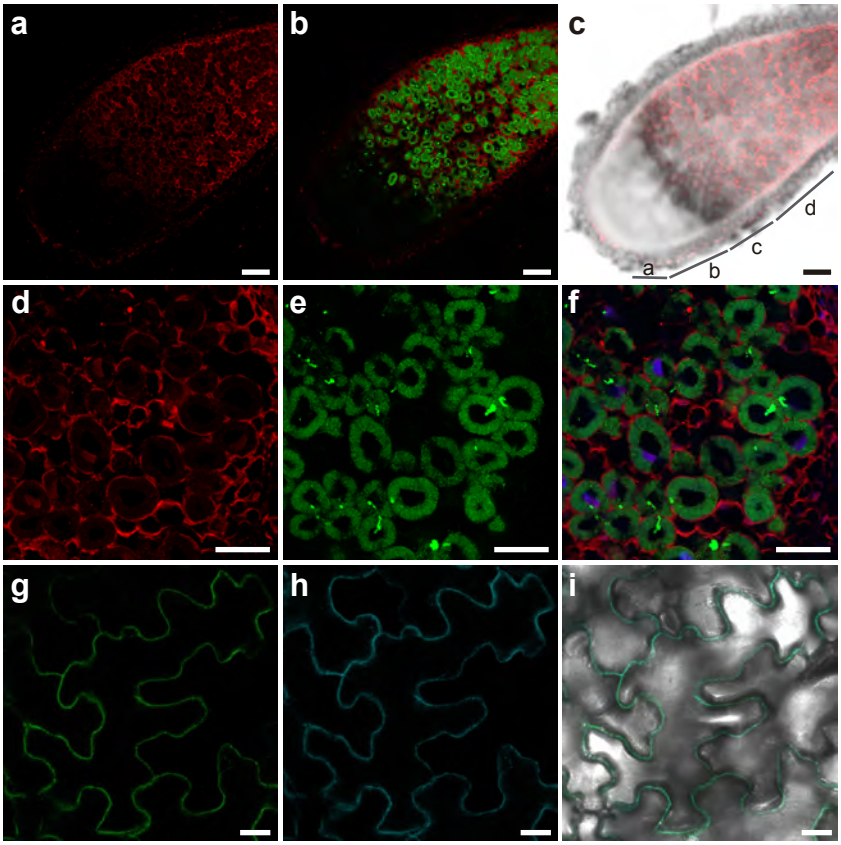

Figure 5

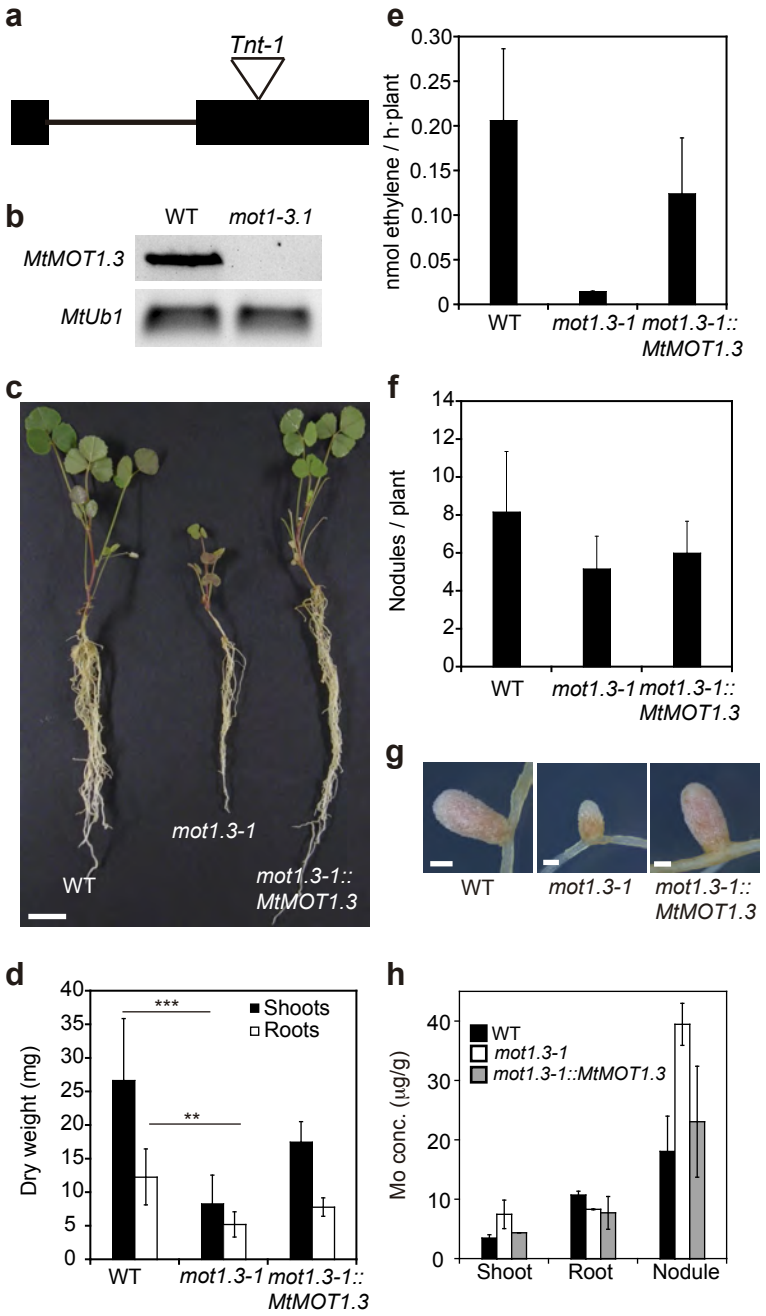
a
Tnt-1
b
WT
mot1-3.1
MtMOT1.3
MtUb1
c
WT
mot1.3-1
mot1.3-1::
MtMOT1.3
d
Dry weight (mg)
Shoots
Roots
***
**
WT
mot1.3-1
mot1.3-1::
MtMOT1.3
e
nmol ethylene / h·plant
WT
mot1.3-1
mot1.3-1::
MtMOT1.3
f
Nodules / plant
WT
mot1.3-1
mot1.3-1::
MtMOT1.3
g
WT
mot1.3-1
mot1.3-1::
MtMOT1.3
h
Mo conc. (µg/g)
WT
mot1.3-1
mot1.3-1::MtMOT1.3
Shoot
Root
Nodule

Figure 6

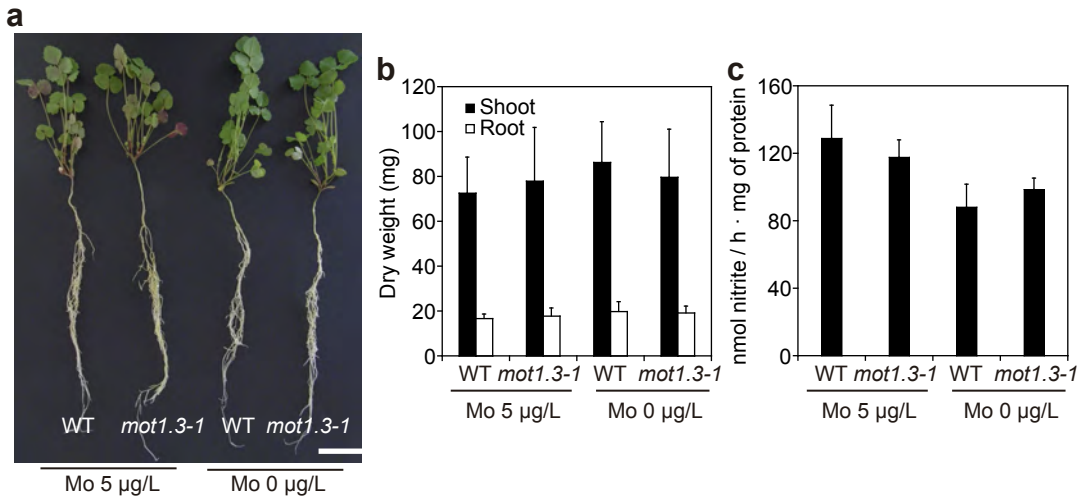
a
WT
mot1.3-1
WT
mot1.3-1
Mo 5 µg/L
Mo 0 µg/L
b
Shoot
Root
Dry weight (mg)
120
100
80
60
40
20
0
WT
mot1.3-1
WT
mot1.3-1
Mo 5 µg/L
Mo 0 µg/L
c
nmol nitrite / h · mg of protein
160
120
80
40
0
WT
mot1.3-1
WT
mot1.3-1
Mo 5 µg/L
Mo 0 µg/L

Figure 7

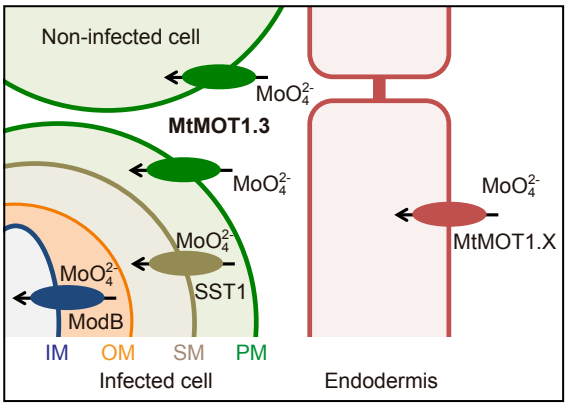
Non-infected cell
MoO_4^{2-}
MtMOT1.3
MoO_4^{2-}
MoO_4^{2-}
SST1
MoO_4^{2-}
ModB
IM
OM
SM
PM
Infected cell
MoO_4^{2-}
MtMOT1.X
Endodermis

Supplemental Methods

Nodule development studies

Sterile seedlings were transferred to plates with Fahreus agar medium (Sauviac et al., 2005) without added molybdate and inoculated with 100 µl of saturated culture of *S. meliloti.* These plants were grown for 28 days at 16 h light and 22 ºC and 8 h darkness and 16 ºC. Morphological analyses were carried out in 28 dpi nodules collected and fixed in 0.25 % glutaraldehyde, 4 % formaldehyde, 2.5 % sucrose in 50 mM potassium phosphate buffer (pH7.4) at 4 ºC. Samples were dehydrated in an ethanol series and embedded in LR-White resin (London Resin Company Ltd, UK). Finally, nodules were placed in gelatin capsules, filled with resin and polymerized at 60 ºC for 24 h. Serial thin sections (0.5 µm) were cut with a Reichert Ultracut microtome (Leica, Vienna, Austria) fitted with a glass knife at the National Center for Electron Microscopy (Universidad Complutense de Madrid, Spain). Sections were stained with 1 % toluidine blue. Direct observation of sections was performed under a Zeis Axiophot photomicroscope (Carl Zeiss, Oberkoche, Germany) with an attached digital camera (Leica DFC 420C, Heerburgg, Switzerland).

Immunohistochemistry and confocal microscopy

The localization of MtMOT1.3-HA was also determined using an anti-mouse Alexa488-conjugated antibody in sections from nodules colonized by a *S. meliloti* strain that constitutively expresses m-Cherry. Nodules and roots were collected at 28-dpi and fixed at 4 ºC overnight in 4 % (w/v) paraformaldehyde and 2.5 % (w/v) sucrose in phosphate-buffered saline (PBS). Fixed plant material was sectioned, 100 µm wide, with a Vibratome 1000 Plus. Cell wall permeabilization was carried out by incubation with 2 % (w/v) cellulase in PBS for 1 h and 0.1 % (v/v) Tween 20 for 15 min. Sections were blocked with 5 % (w/v) bovine serum albumin in PBS and then incubated with 1:50 anti-HA mouse monoclonal antibody (Sigma) in PBS at room temperature for 2 h. Primary antibody was washed three times with PBS for 10 min and subsequently incubated with 1:40 Alexa4884-conjugated anti-mouse rabbit monoclonal antibody (Sigma) in PBS at room temperature for 1 h. Secondary antibody was washed three times with PBS for 10 min, and then DNA was stained using DAPI. Images were obtained with a confocal laser-scanning microscope (Leica SP8).

Western blot

Total root and nodule protein extracts were obtained from *M. truncatula* wild-type and from transformants expressing *MtMOT1.3-HA* as described by Larrainzar et al. (Larrainzar et al., 2007). Briefly, 100 mg fresh weight of nodules or roots was homogeneized in a mortar with liquid nitrogen and resuspended in cold extraction buffer (25 mM MES, 450 mM mannitol, 7 mM EDTA, 7 mM $CaCl_2$, 5 mM $MgCl_2$, 20 mM ascorbic acid, 10 mM ditithreitol pH7.2). Homogenates were briefly centrifuged at 500 x g for 5 min to remove cell debris. Protein determination was performed in accordance to Bradford (Bradford, 1976). 25 µg of this crude extract was loaded in SDS-PAGE gels (Laemmli, 1970), and protein bands visualized with Coomassie Brilliant Blue. HA-labelled proteins were detected by electroblotting the gels onto nitrocellulose membranes and immunostaining with a primary anti-HA mouse antibody (1:1000, Sigma) and a horseradish peroxidase-conjugated anti HA rabbit antibody (1:1000, Agrisera).

Bradford MM. 1976. A rapid and sensitive method for the quantitation of microgram quantities of protein utilizing the principle of protein-dye binding. *Analytical Biochemistry* **7**: 248-254.

Laemmli UK. 1970. Cleavage of structural proteins during the assembly of the head of bacteriophage T4. *Nature* **227**: 680-685.

Larrainzar E, Wienkoop S, Weckwerth W, Ladrera R, Arrese-Igor C, González EM. 2007. *Medicago truncatula* root nodule proteome analysis reveals differential plant and bacteroid responses to drought stress. *Plant Physiology* **144**: 1495-1507.

Sauvia L, Niebel A, Boisson-Dernier A, Barker DG, de Carvalho-Niebel F. 2005. Transcript enrichment of Nod factor-elicited early nodulin genes in purified hair fractions of model legume *Medicago truncatula*. *Journal of Experimental Botany* **56**: 2507-2513.

Table S1. Primers used in this study

Name	Sequence (5' - 3')	Use
5MtMOT1.1+2087QF	CCATTTGGAACCAGAAAAGTCCA	Quantitative expression of *MtMOT1.1*
3MtMOT1.1+2234QR	GAACCCTAGCAAGACCTCACA	Quantitative expression of *MtMOT1.1*
5MtMOT1.2+1689QF	GACCGAACTTTGCAGAAAGCA	Quantitative expression of *MtMOT1.2*
3MTMOT1.2+1813QR	TGGGGATTTGGCTTGTCATCA	Quantitative expression of *MtMOT1.2*
5MTMOT1.3+1077QF	TTGTCATGGTGCCGGTGGAC	Quantitative expression of *MtMOT1.3*
3MTMOT1.3+1237QR	ACACTCCTAAGATCCCGACCGACCG	Quantitative expression of *MtMOT1.3*
5MTMOT1.4QF	CACACGACAACATCTCCAACGACCAACC	Quantitative expression of *MtMOT1.4*
3MTMOT1.4QR	AAGGTTGTTGACTAGTGATAAGGC	Quantitative expression of *MtMOT1.4*
5MTMOT1.5+1260QF	CTTGTGGGGTCTAGTGCTGC	Quantitative expression of *MtMOT1.5*
3MTMOT1.5+1367QR	ACTTGCTCTTGACCTTCATGC	Quantitative expression of *MtMOT1.5*
35MtUBqF	GAACTTGTTGCATGGGTCTTGA	Quantitative expression of *MtUbiquitin carboxyl-terminal hydrolase*
3MtUBqR	CATTAAGTTTGACAAAGAGAAAGAGACAGA	Quantitative expression of *MtUbiquitin carboxyl-terminal hydrolase*
5MTMOT13F	AAAACTGCAGCATTTTATTTTCTTCCATTGGTTC	*MtMOT1.3* cDNA cloning into pDR196
3MTMOT13_534R	AAAACTCGAGAAATTGCCATATTTTTGAAATCCC	*MtMOT1.3* cDNA cloning into pDR196
5MtMOt13-1085pGW	GGGGACAAGTTTGTACAAAAAAGCAGGCTAAAT-GACATATTTGCATAAAATTGG	*MtMOT1.3* promoter cloning into pGWB3 or pGWB13 vectors

5MtMOT13p2000GW	GGGGACAAGTTTGTACAAAAAAGCAGGCTAGTG-CATAGACAACATCAAAAAGC	*MtMOT1.3* promoter cloning into pGWB3 vector
3MtMOT13+1441GW	GGGGACCACTTTGTACAAGAAAGCTGGGTAGAT-GAGGCTTTTCTGATTCCAAAT	*MtMOT1.3* genomic region cloning into pGWB13 or pGWB5 vectors
5MtMOT12+1GW-C	GGGGACAAGTTTGTACAAAAAAGCAGGCTATGG-AAAACCAAAACCCTCC	

Table S2. Occurrence of MOT1 members in the genome of legume and non-legume plants.

Legumes	Members of the MOT1 family
Arachis duranensis	3
Cajanus cajan	3
Cicer arietinum	4
Glycine max	9
Medicago truncatula	5
Phaseolus vulgaris	4
Pisum sativum	4
Vigna angularis	5
Average	4.62
Non-legume plants	
Arabidopsis thaliana	2
Hordeon vulgare	2
Populus trichocarpa	2
Ricinus communis	3
Solanum tuberosum	2
Sorghum bicolor	3
Vitis vinifera	2
Zea mays	2
Average	2.25

Figure S1. Determination of MOT1 gene family expression in nodulated and nitrogen-fertilized *M. truncatula* plants relative to the to the internal standard gene *Ubiquitin carboxyl-terminal hydrolase*. Data are the mean ± SD of two independent experiments with 4 pooled plants. n.d., non-detected.

Figure S2. Determination of *MtMOT1.3* regulation by molybdate relative to the internal standard gene *Ubiquitin carboxyl-terminal hydrolase*. Data are the mean ± SD of three independent experiments with 4 pooled plants each.

Figure S3. Growth of *S. cerevisiae* transformed with pDR196 or with pDR196 expressing MtMOT1.3 under different concentrations of sodium molybdate. (a) 0 µM added sodium molybdate. (b) 10 µM added sodium molybdate. (c) 30 µM added sodium molybdate.(d) 50 µM added sodium molybdate. (e) 100 µM added sodium molybdate. (f) 1000 µM added sodium molybdate. Data are the mean ± SD of two independent experiments.

Figure S4. Autofluorescence control for Alexa594 emission. Immunolocalization of MtMOT1.3-HA in nodule sections from 28 dpi *M. truncatula* plants transformed with pGWB13::MtMOT1.3-HA. Left nodule was incubated with a mouse anti-HA antibody, while just PBS was used for the right one. The image is the result of a z-project of 22 optical sections combining a tilescan of 14 areas.

Figure S5. MtMOT1.3 is localized in the plasma membrane. Cross section of a 28 dpi *M. truncatula* nodule expressing MtMOT1.3-HA and infected with a S. *meliloti* strain constitutively expressing mCherry (red). DNA is stained with DAPI (blue). (a) Nodule section incubated with an anti-HA mouse antibody and a anti-mouse Alexa488-conjugated antibody (green). Left panel differential interface contrast image; top middle panel, S. meliloti distribution; lower middle panel, DNA distribution; top right panel MtMOT1.3-HA distribution; lower right panel overlay of DAPI, mCherry, and Alexa488 signals. Bars = 10 µm. (b) Nodule section prepared as in (a) but not adding the anti-HA mouse antibody. Top left panel, S. meliloti distribution; lower left panel, DNA distribution; top right panel distribution of Alexa488 signal; lower right panel differential interface contrast image. Bars = 20 µm.

Figure S6. Immunolocalization of MtMOT1.3-HA in crude protein extracts from 28-dpi *M. truncatula* roots and nodules obtained from control and pGWB13::MtMOT1.3-HA transformed plants.

32 Figure S7. Transient expression of MtMOT1.3-GFP in *N. benthamiana* leaves. (a) to (c)
33 Plasma membrane marker-CFP expression. (a) Plasma membrane marker-CFP signal in
34 the green channel. (b) Plasma membrane marker-CFP in the cyan channel. (c) Overlay of
35 green and cyan channels and differential interference contrast. Bars = 25 µm. (d) to (f)
36 MtMOT1.3-GFP expression. (d) MtMOT1.3-GFP signal in the green channel. (e)
37 MtMOT1.3-GFP signal in the cyan channel. (f) Overlay of green and cyan channels and
38 differential interference contrast. Bars = 25 µm.

39 Figure S8. Nitrogenase activity in 28-dpi nodules. Acetylene reduction was measured in
40 duplicate from two sets of four pooled plants. Data are the mean ± SD.

41 Figure S9. Nodule development in wild type and mot1.3-1 plants. Logitudinal sections of
42 wild type (a) and mot1.3-1 (b) nodules stained with toluidine blue. Bars = 100 µm. (c)
43 Nodule growth in wild type and mot1.3-1 plants. Bars = 100 µm (d) Nodulation kinetics
44 in wild type and mot1-3 plants. Data are the mean ± SD from ten plants.

45 Figure S10. *mot1.3-1* mutant aberrant phenotype is restored upon supplementation with
46 molybdate. (a) Growth of representative plants of wild type and *mot1.3-1* mutant. Bar =
47 3 cm. (b) Dry weight of shoots and roots. Data are the mean ± SD of at least 6 independent
48 plants. Asterisk indicates significant differences: *$p < 0.05$, **$p < 0.01$. (c) Number of
49 nodules per plant. Data are the mean ± SD of at least 6 independent plants. (d) Nitrogenase
50 activity in 28-dpi nodules. Acetylene reduction was measured in duplicate from two sets
51 of four pooled plants. Data are the mean ± SD. Asterisk indicates significant differences:
52 *$p < 0.05$. (e) Nodule length in 28-dpi nodules. Data are the mean ± SD of 15 nodules
53 from from 6 plants. Asteriks indicates significant differences: *$p < 0.05$.

54 Figure S11. *mot1.3-1* plants show reduced nitrogenase activity also in hydroponics. (a)
55 Growth of representative plants of wild type and mot1.3-1 mutant. Bar = 3 cm. (b) Dry
56 weight of shoots and roots. Data are the mean ± SD of at least 8 independent plants.
57 Asterisk indicates signifi-cant differences: *$p < 0.05$, **$p < 0.01$. (c) Number of nodules
58 per plant. Data are the mean ± SD of at least 7 independent plants. (d) Nitrogenase activity
59 in 28-dpi nodules. Acetylene reduction was measured in duplicate from two sets of four
60 pooled plants. Data are the mean ± SD. Asterisk indicates significant differences: *$p <$
61 0.05

62 Figure S12. Expression of *MtMOT1.1, MtMOT1.2, MtMOT1.4,* and *MtMOT1.5* in
63 *mot1.3-1* nodules relative to the internal standard gene *Ubiquitin carboxyl-terminal*

64 *hydrolase* and relativised to the expresion value in wild type plants (100 %). Data are the
65 mean ± SD of three independent experiments with 4 pooled plants each.

Figure S1

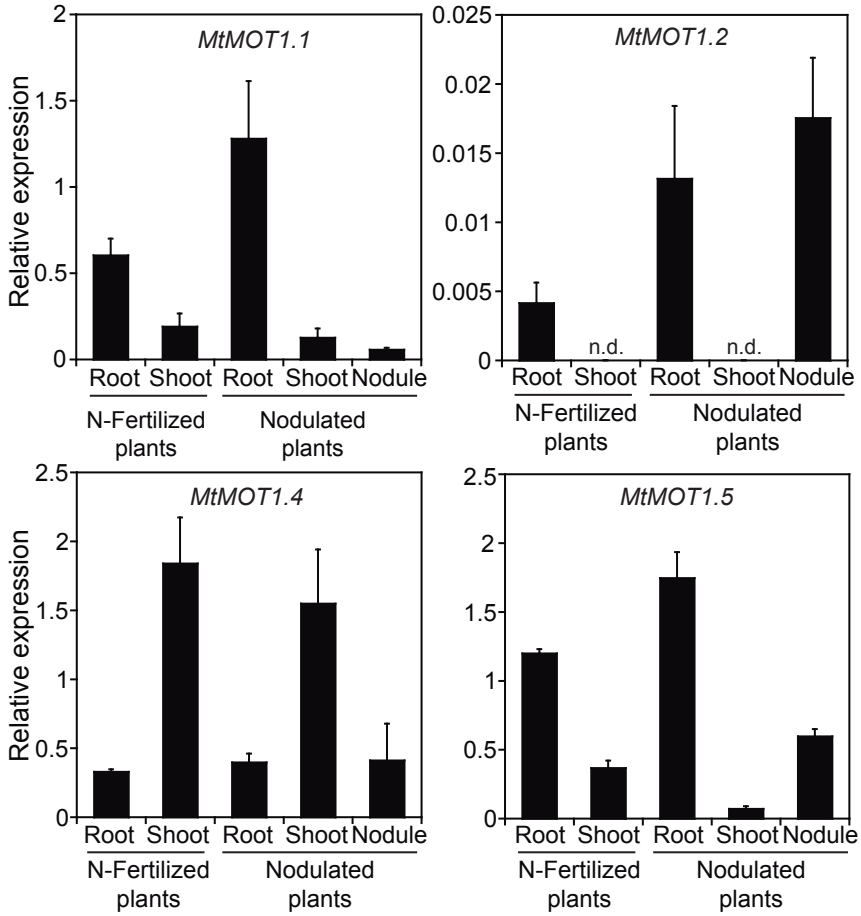
MtMOT1.1
MtMOT1.2
MtMOT1.4
MtMOT1.5
Relative expression
Root
Shoot
Nodule
n.d.
N-Fertilized plants
Nodulated plants

Figure S2

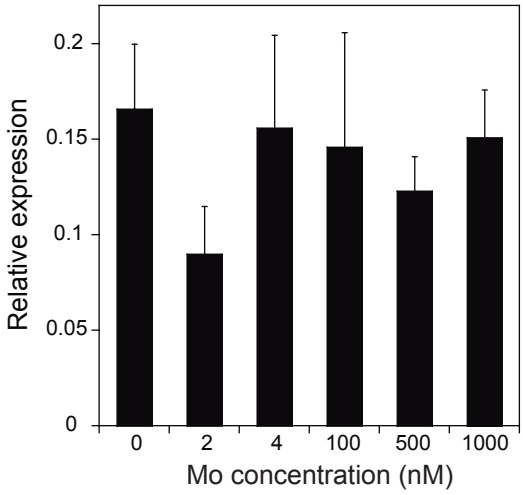
Relative expression
0.2
0.15
0.1
0.05
0
0
2
4
100
500
1000
Mo concentration (nM)

Figure S3

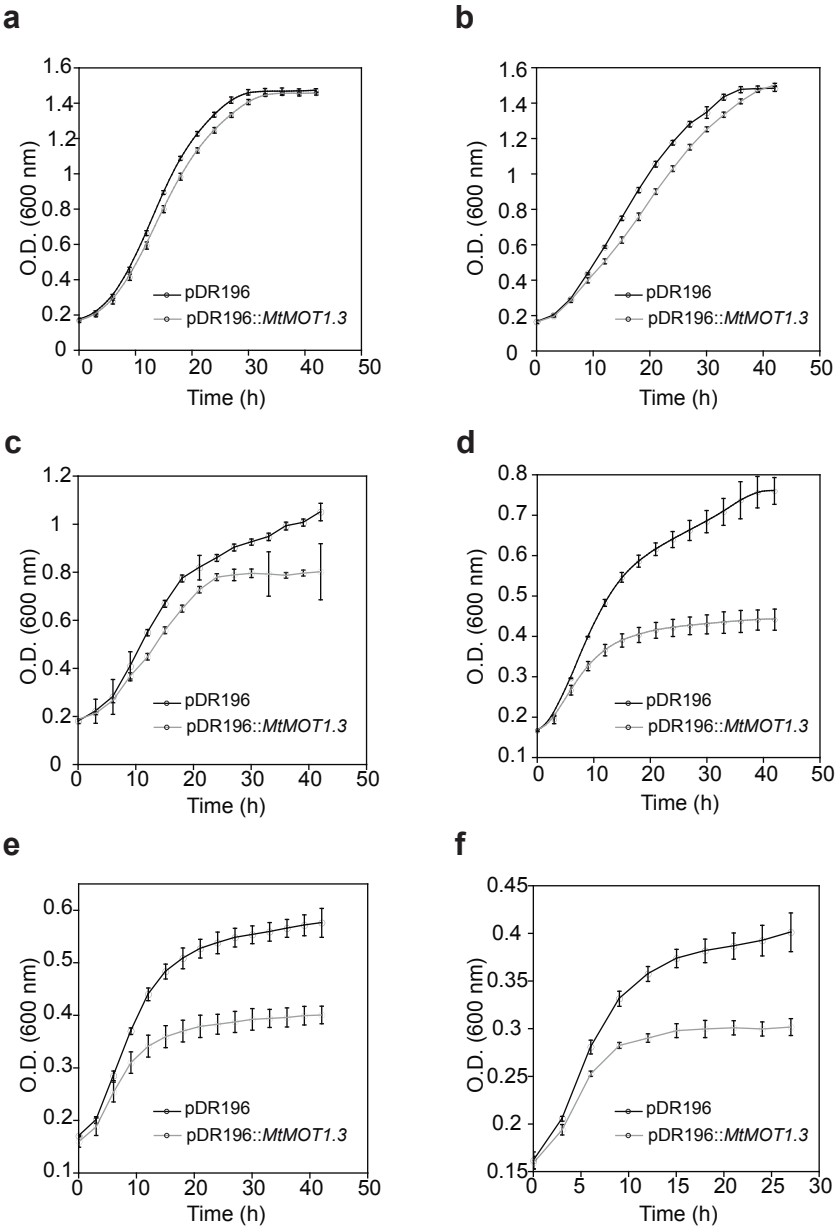

Figure S4

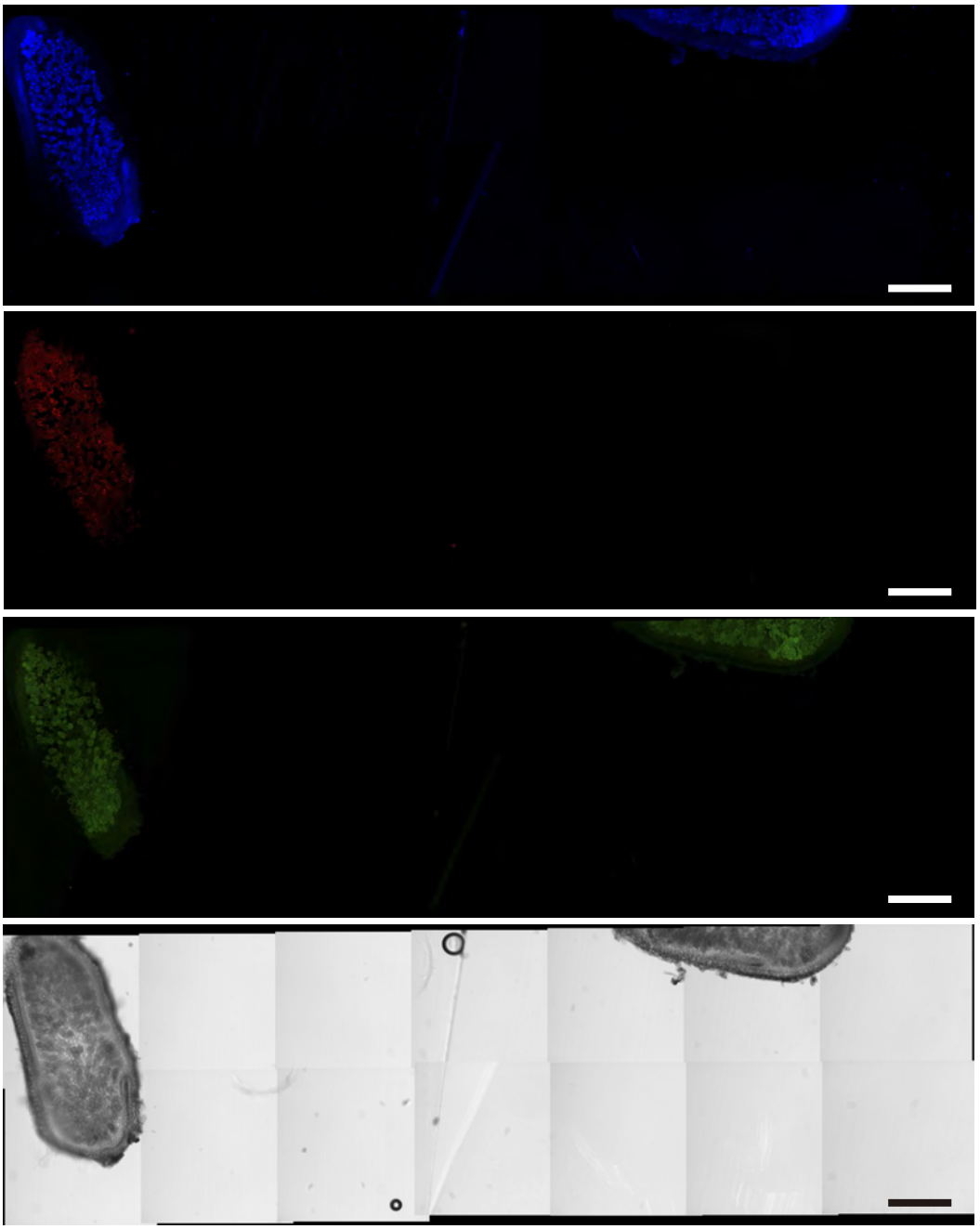

Figure S5

a

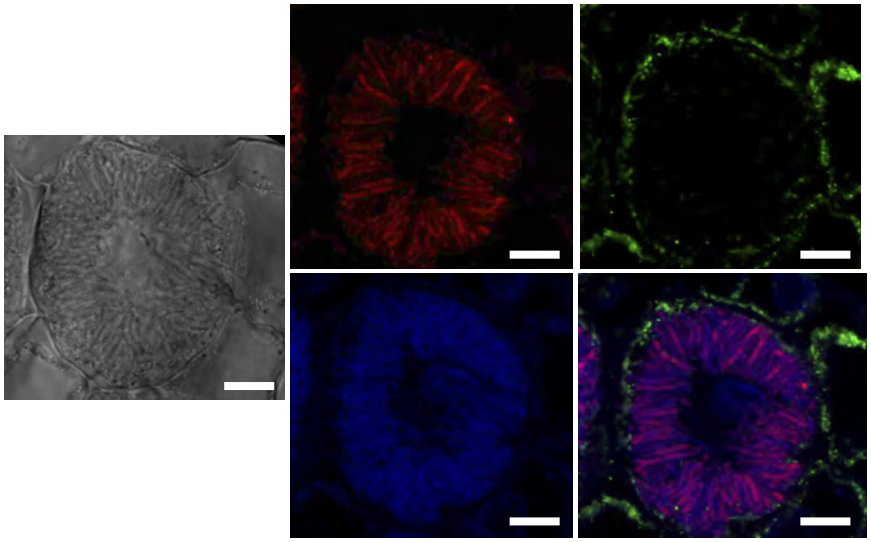

b

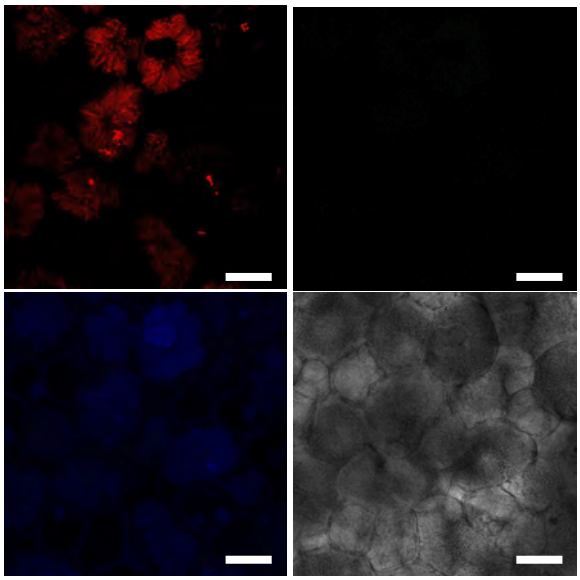

Figure S6

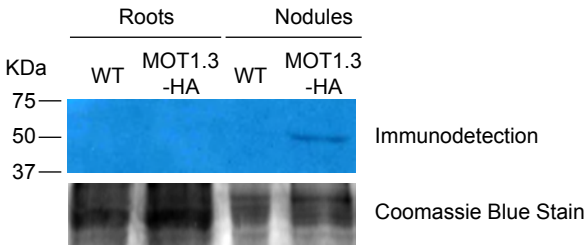
Roots
Nodules
KDa
WT
MOT1.3
-HA
WT
MOT1.3
-HA
75
50
37
Immunodetection
Coomassie Blue Stain

Figure S7

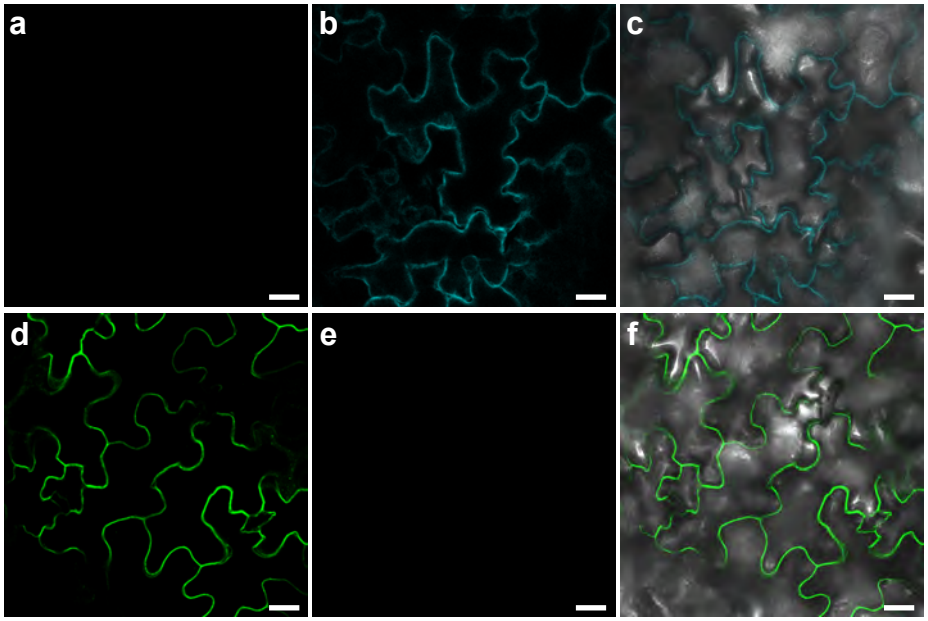

Figure S8

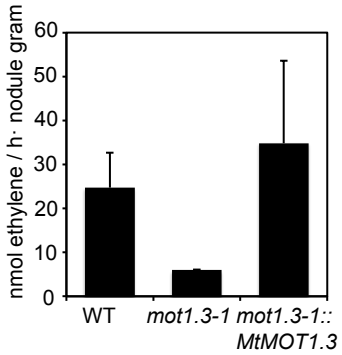
nmol ethylene / h· nodule gram
60
50
40
30
20
10
0
WT
mot1.3-1
mot1.3-1::
MtMOT1.3

Figure S9

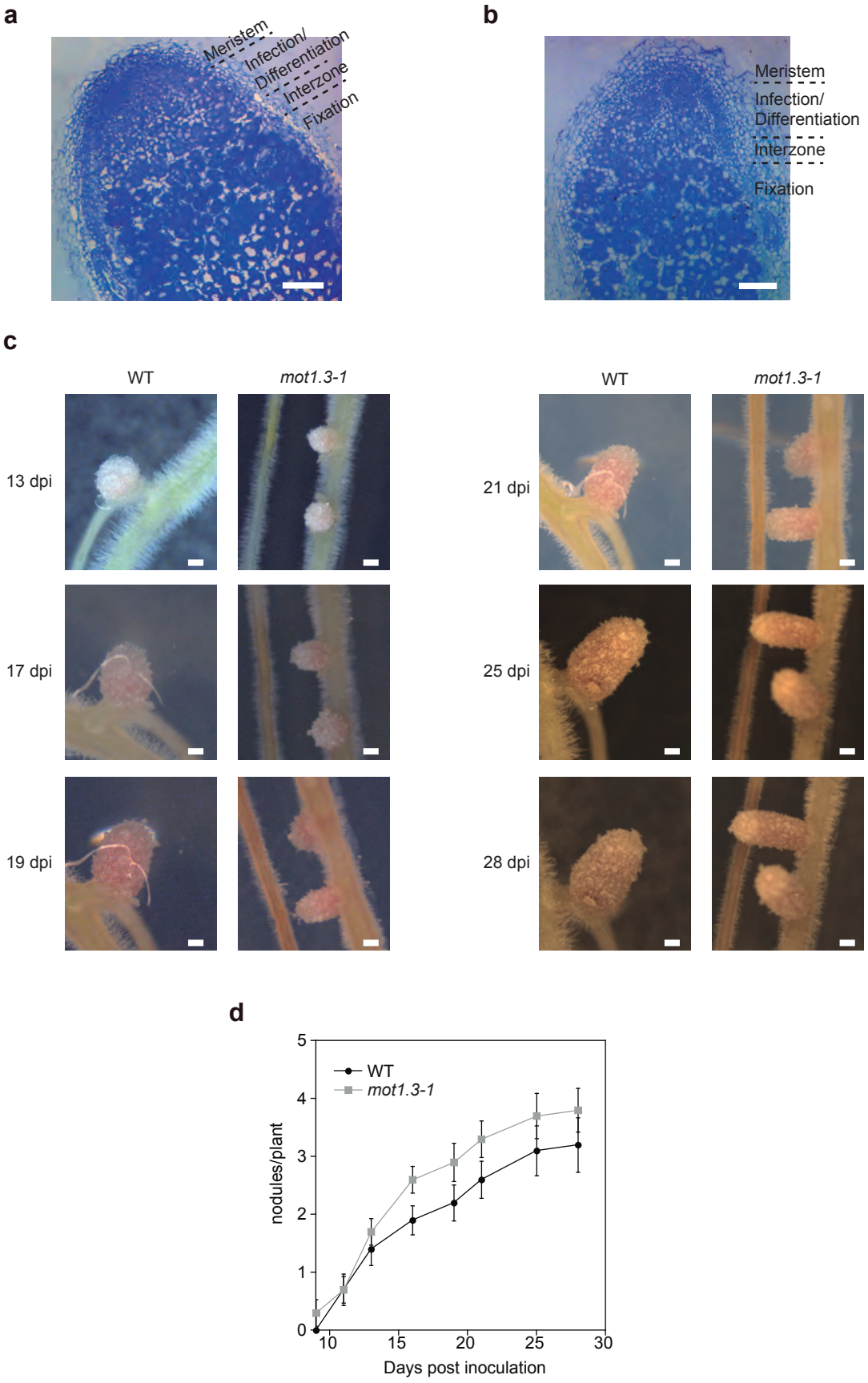
a
Meristem
Infection/
Differentiation
Interzone
Fixation
b
Meristem
Infection/
Differentiation
Interzone
Fixation
c
WT
mot1.3-1
13 dpi
17 dpi
19 dpi
WT
mot1.3-1
21 dpi
25 dpi
28 dpi
d
WT
mot1.3-1
nodules/plant
Days post inoculation
0
1
2
3
4
5
10
15
20
25
30

Figure S10

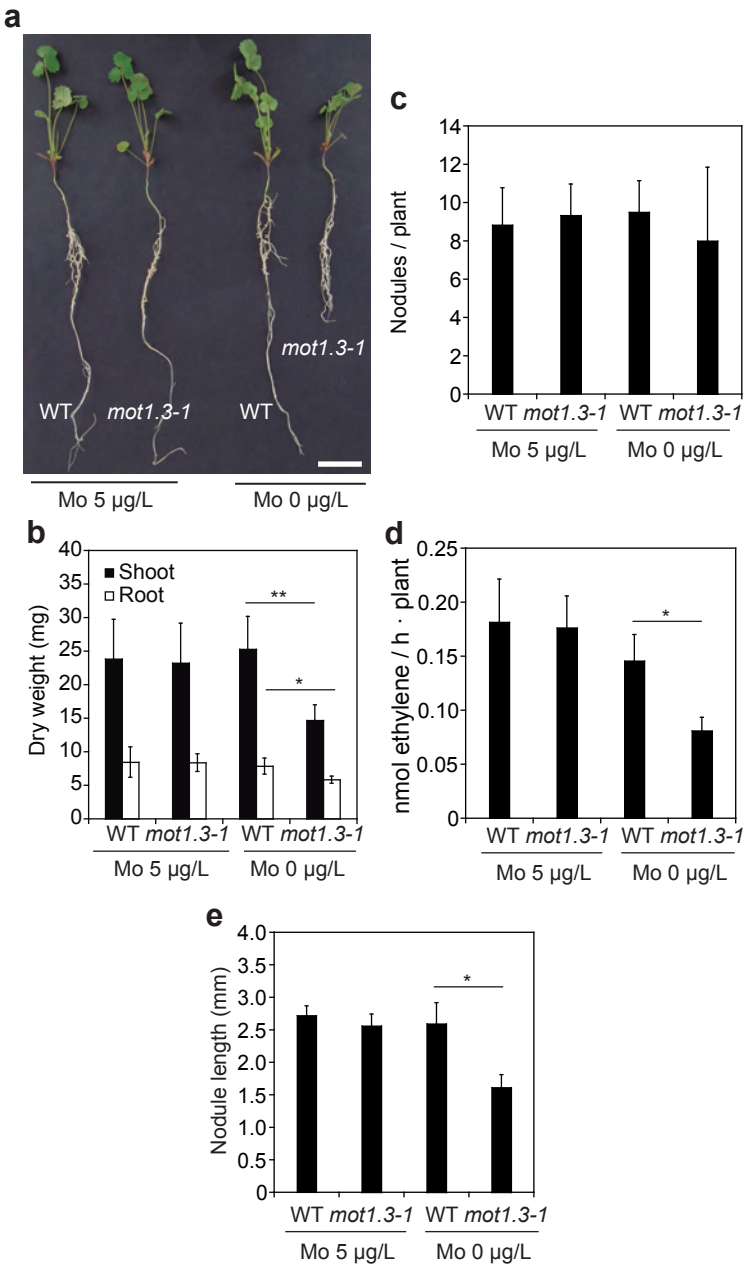
a
WT
mot1.3-1
WT
mot1.3-1
Mo 5 µg/L
Mo 0 µg/L
b
Shoot
Root
Dry weight (mg)
40
35
30
25
20
15
10
5
0
**
*
WT mot1.3-1 WT mot1.3-1
Mo 5 µg/L
Mo 0 µg/L
c
Nodules / plant
14
12
10
8
6
4
2
0
WT mot1.3-1 WT mot1.3-1
Mo 5 µg/L
Mo 0 µg/L
d
nmol ethylene / h · plant
0.25
0.20
0.15
0.10
0.05
0
*
WT mot1.3-1 WT mot1.3-1
Mo 5 µg/L
Mo 0 µg/L
e
Nodule length (mm)
4.0
3.5
3.0
2.5
2.0
1.5
1.0
0.5
0
*
WT mot1.3-1 WT mot1.3-1
Mo 5 µg/L
Mo 0 µg/L

Figure S11

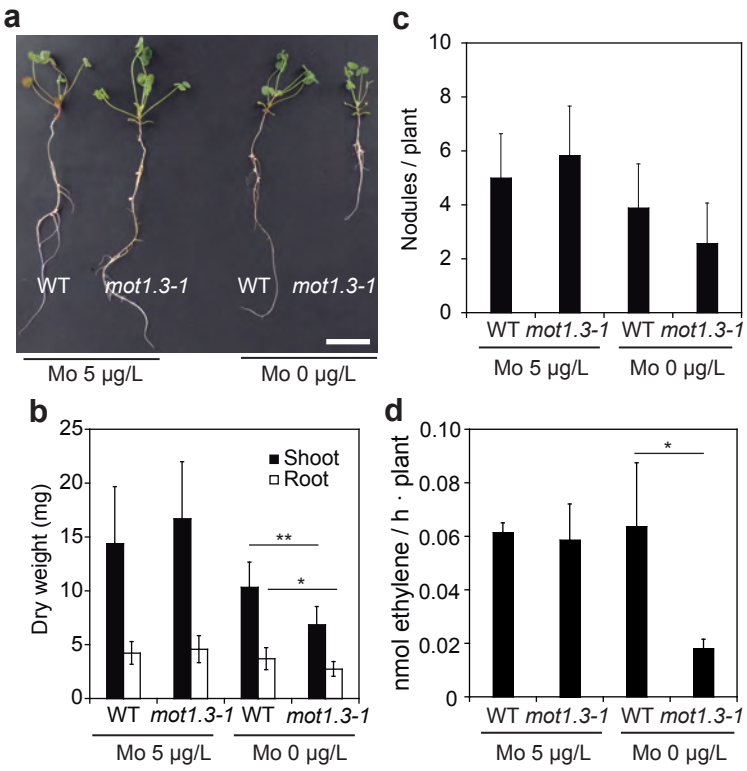
a
WT
mot1.3-1
WT
mot1.3-1
Mo 5 µg/L
Mo 0 µg/L
c
Nodules / plant
10
8
6
4
2
0
WT mot1.3-1 WT mot1.3-1
Mo 5 µg/L
Mo 0 µg/L
b
Dry weight (mg)
25
20
15
10
5
0
Shoot
Root
**
*
WT mot1.3-1 WT mot1.3-1
Mo 5 µg/L
Mo 0 µg/L
d
nmol ethylene / h · plant
0.10
0.08
0.06
0.04
0.02
0
*
WT mot1.3-1 WT mot1.3-1
Mo 5 µg/L
Mo 0 µg/L

Figure S12

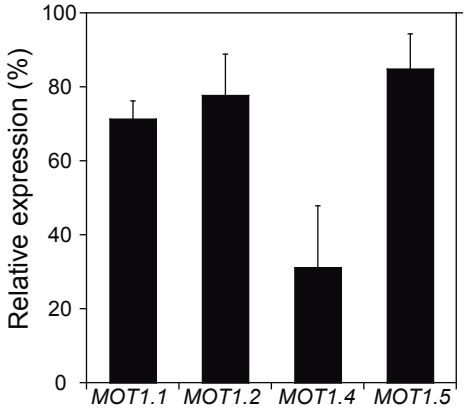
Relative expression (%)
100
80
60
40
20
0
MOT1.1
MOT1.2
MOT1.4
MOT1.5